

RESEARCH

Open Access



# IDO1 modulates pain sensitivity and comorbid anxiety in chronic migraine through microglial activation and synaptic pruning

Jiao Hu<sup>1,2†</sup>, Wen-Juan Ji<sup>1,2†</sup>, Gui-Yu Liu<sup>1,2†</sup>, Xiao-Hong Su<sup>3</sup>, Jun-Ming Zhu<sup>1,2</sup>, Yu Hong<sup>1</sup>, Yi-Fan Xiong<sup>1</sup>, Yun-Yan Zhao<sup>4\*</sup>, Wei-Peng Li<sup>1,2,5\*†</sup> and Wei Xie<sup>1,2\*</sup>

## Abstract

**Background** Chronic migraine is a prevalent and potentially debilitating neurological disorder that is often comorbid with mental health conditions (such as anxiety and depression), but the underlying mechanisms linking these conditions remain poorly understood. Indoleamine 2,3-dioxygenase 1 (IDO1) has been implicated in inflammatory processes, including neuroinflammation and pain. However, its role as a link between neuroinflammation and pain sensitization in chronic migraine is not well defined.

**Methods** Male mice were used to establish a model of chronic migraine by recurrent intraperitoneal injections of nitroglycerin (NTG, 10 mg/kg). Using pharmacological approaches, transgenic strategies and adeno-associated virus (AAV) intervention, we investigated the role of IDO1 in pain sensitization and migraine-related mood disorders in an NTG-induced chronic migraine mouse model. We employed a combination of immunoblotting, immunohistochemistry, three-dimensional reconstruction, RNA sequencing, electrophysiology, in vivo fiber photometry, and behavioral assays to elucidate the underlying mechanisms involved.

**Results** Our findings demonstrated that pharmacological inhibition and genetic knockout of IDO1 significantly alleviated pain sensitivity in a chronic migraine model. Neuronal activity in the anterior cingulate cortex (ACC) was evaluated with in vitro c-Fos immunostaining as well as in vivo fiber photometry, and a shift in the excitation/inhibition (E/I) balance toward excitation was observed through whole-cell patch clamp recording. Notably, IDO1 expression was increased in the ACC, and AAV-mediated IDO1 knockdown in the ACC rescued pain sensitivity, electrophysiological E/I balance changes, and anxiety-like behavior in chronic migraine model mice. Furthermore, IDO1 regulated microglial activation and pruning of neuronal synapses in the ACC. IDO1's microglial pruning function

<sup>†</sup>Jiao Hu, Wen-Juan Ji, Gui-Yu Liu and Wei-Peng Li contributed equally to this work as co-first authors.

\*Correspondence:

Yun-Yan Zhao

z-y-y116@163.com

Wei-Peng Li

wp\_lee@smu.edu.cn

Wei Xie

xieweizn@smu.edu.cn

Full list of author information is available at the end of the article



© The Author(s) 2025. **Open Access** This article is licensed under a Creative Commons Attribution-NonCommercial-NoDerivatives 4.0 International License, which permits any non-commercial use, sharing, distribution and reproduction in any medium or format, as long as you give appropriate credit to the original author(s) and the source, provide a link to the Creative Commons licence, and indicate if you modified the licensed material. You do not have permission under this licence to share adapted material derived from this article or parts of it. The images or other third party material in this article are included in the article's Creative Commons licence, unless indicated otherwise in a credit line to the material. If material is not included in the article's Creative Commons licence and your intended use is not permitted by statutory regulation or exceeds the permitted use, you will need to obtain permission directly from the copyright holder. To view a copy of this licence, visit <http://creativecommons.org/licenses/by-nc-nd/4.0/>.

appears to be mediated through the interferon (IFN) signaling pathway, and the behavioral changes induced by IDO1 knockdown in the ACC could be reversed by activating this pathway.

**Conclusions** Our findings revealed that microglial IDO1 in the ACC drives pain sensitization and anxiety in chronic migraine, highlighting IDO1 as a potential therapeutic target for chronic migraine treatment.

**Keywords** Indoleamine 2,3-dioxygenase 1 (IDO1), Chronic migraine, Anterior cingulate cortex (ACC), Synapse, Microglia, Excitation/inhibition balance

## Introduction

Migraine is a common and disabling primary headache disorder characterized by recurrent attacks of moderate or severe pain, which can be accompanied by a variety of neurological, gastrointestinal and autonomic symptoms [1, 2]. According to the Global Burden of Disease Study (2021), migraine affects 1.16 billion people and is the third leading cause of disability-adjusted life years [3]. Up to 5% of patients with episodic migraine may progress to chronic migraine, experiencing more intense and prolonged headaches, a higher incidence of comorbidities, and reduced therapeutic effectiveness [1, 4]. Chronic migraine is liable to accompany a wide range of psychiatric comorbidities, particularly anxiety and depression [5, 6]. Despite advances in understanding migraine, current studies have focused mainly on the trigeminal ganglion and trigeminal nucleus caudalis [7–10], which do not fully explain the accompanying symptoms. The mechanisms underlying chronic migraine and its association with these comorbidities remain unclear.

Human brain-imaging studies have identified cortical regions implicated in pain processing, with the anterior cingulate cortex (ACC) emerging as a pivotal area [11]. The ACC is involved in higher-level brain functions including nociception, chronic pain, and emotional processing. Notably, structural and functional changes in the ACC have been observed in migraine patients [12–14]. However, the specific mechanisms linking ACC to the sensory and emotional aspects of chronic migraine remain unclear.

Clinical studies have reported altered tryptophan catabolism and kynurenine metabolism pathways in migraine patients [15, 16]. Indoleamine 2,3-dioxygenase 1 (IDO1) is an intracellular enzyme that catalyzes the initial and rate-limiting step in the degradation of tryptophan via the kynurenine pathway, producing bioactive molecules, including kynurenine and its downstream metabolite quinolinic acid. The expression of IDO1 is observed in peripheral tissues, including macrophages and dendritic cells, as well as in microglia within the central nervous system [17]. IDO1 is normally upregulated by inflammatory mediators, and its most important inducer is the cytokine interferon- $\gamma$  (IFN- $\gamma$ ) [17, 18], which is implicated in several inflammation-related diseases, including tumors, autoimmune disorders and

neurological diseases [19]. Recently, increased attention has been given to investigating the role of IDO1 in neuroinflammation, such as Parkinson's disease, Alzheimer's disease and epilepsy [20–22]. In addition, several studies have reported a critical role of IDO1 in regulating pain hypersensitivity in chronic pain [23–25], suggesting that IDO1 might also be involved in the immune-inflammatory pathogenesis, manifestation, and progression of migraine. However, it remains unclear whether altered IDO1 expression contributes to migraine, or whether it represents a consequence of chronic migraine.

In this study, we employed pharmacological inhibition, genetic knockout, and adeno-associated virus (AAV)-mediated knockdown to investigate the role of IDO1 in chronic migraine and its mood comorbidities. Using *in vivo* fiber photometry and whole-cell patch-clamp techniques, we detected an increase in neuronal activity that affected the excitation/inhibition (E/I) balance in the ACC. Our findings revealed that microglial IDO1 mediates the regulation of neuronal synaptic transmission and pain sensitization. This alteration is mediated by microglial activation and synaptic pruning through the IFN signaling pathway. Overall, our study provides novel insights into the molecular and cellular mechanisms underlying chronic migraine, highlighting the pivotal role of IDO1 in modulating pain sensitivity and associated comorbidities through its effects on microglial function and synaptic integrity.

## Methods and materials

### Animals

Male C57BL/6J mice (18–22 g, aged 6–8 weeks) were purchased from the Experimental Animal Center of Southern Medical University (Guangzhou, China). IDO1 knockout (KO) mice (strain #:005867) were obtained from the Jackson Laboratory (Bar Harbor, ME, USA), and wild-type (WT) littermates were produced by heterozygous mating. Genotyping was performed using PCR with the following three primers: (1) Mutant forward: CGT GCA ATC CAT CTT GTT CA, (2) WT forward: TAT TGA AAG GGG AAT CCA GA, (3) Common: GTG TCA GAA AGC TCA CTG CTT. Male homozygous mice and WT littermates were used for experiments. All animals were housed in groups of 3–5 per cage with free access to food and water and maintained on a 12 h light/dark cycle

with controlled room temperature and humidity. Mice were randomized into different treatment groups, and all experimental analyses were conducted by an investigator blinded to the treatment group. All animal experimental procedures were approved by the Institutional Animal Care and Use Committee of Southern Medical University (L-2019-071, Guangdong, China).

#### **Drug administration**

The nitroglycerin (NTG) (Beijing Yimin, H11020289) stock solution, a concentration of 5.0 mg/ml was freshly diluted to 1 mg/ml with 0.9% saline before each injection. Mice received intraperitoneal injections of 10 mg/kg NTG or vehicle every other day for 9 days.

As described in our previous study [26], mice were pre-treated with subcutaneous administration of 50 mg/kg IDO1 antagonist 1-methyltryptophan(1-MT) (Bidepharm, BD30153) or vehicle (1% DMSO in 0.9% NaCl) every day.

Additionally, mice were received daily intraperitoneal injection of 30 mg/kg IFN agonist tilorone dihydrochloride (Bidepharm, BD154145) or vehicle (0.9% NaCl) [27].

#### **Animal models of chronic migraine**

##### **NTG-induced chronic migraine mouse model**

According to previous report [28], mice were received intraperitoneal injections of 10 mg/kg NTG every other day for 5 times to establish a mouse model with chronic migraine. Control group mice received isovolumic saline injections. Pain threshold tests were performed before and 2 h after each vehicle/NTG injection to measure basal and acute responses, respectively (Fig. 1A).

##### **Induction of cortical spreading depression (CSD)**

Potassium chloride (KCl) was used to induce CSD in the chronic migraine model, based on a previous report [29]. Briefly, a 1.5 mm burr hole was drilled above the ACC (1.2 mm anterior and 0.25 mm bilateral to Bregma) in mice, and CSDs were evoked by placing a cotton ball soaked with 1 M KCl over the dura for 1 h, every other day for 5 times (Supplementary Fig. 4A).

##### **Electrical stimulation (ES)-induced chronic migraine mouse model**

ES-induced chronic migraine model was established accordingly [30]. Briefly, two screws (1 mm diameter) were placed onto the dural surface through drilled holes and attached to the skull using glass ionomer cement. After a 7-day recovery period, mice received ES (1 h, 5 Hz, 0.5 ms pulse duration, and 1 mA intensity) every other day for 5 times. Sham group were connected to the stimulator without stimulation for 1 h (Supplementary Fig. 4B).

##### **Reserpine-induced chronic migraine mouse model**

For reserpine-induced chronic migraine model [31], mice were received intraperitoneal injection with reserpine (Sigma-Aldrich, 83580) at a dose of 1 mg/kg once daily for 10 days. Control group mice receiving injections of isovolumic saline (Supplementary Fig. 4C).

#### **Behavioral experiments**

Mice were handled for 3 consecutive days before behavioral experiments to ensure familiarization to the investigator and to minimize stress, and acclimatized to the experimental room for at least 2 h before all behavioral tests. All behavioral tests were performed in a quiet, moderately lit (100 lx) standard behavioral testing room separate from the housing room. The experimenter was blinded to group identity during the experiment and quantitative analyses.

##### **Mechanical sensitivity measurements**

Mechanical thresholds were quantitatively assessed by stimulating the hind paw with von Frey filament. Mice were placed in individual clear acrylic chambers with wire mesh platform through which the von Frey hairs (Danmic Aesthesio, USA) were applied. The 50% paw withdrawal threshold was determined by using the “up-down” method as described previously [32]. The force of filament strength utilized for measuring the mechanical threshold in the hind paws of mice spans from 0.008 g to 2.0 g, with an initial filament application of 0.4 g, maintaining a consistent force for 5–6 s. The strength of the subsequent filament (0.6 g) was increased when mice absent response, while decreased the filament (0.16 g) when mice exhibited response (sharply paw withdrawal, licking or shaking of hind paw), and so on. The stimuli were presented with a minimum interval of 30 s to prevent sensitization following successive filament applications. Four times measurements were applied after the first positive response was occurred, then the up-down procedure was stopped.

##### **Thermal sensitivity measurements**

Thermal thresholds were evaluated using the hot plate test [33]. The temperature of the hot plate apparatus was maintained at  $55 \pm 0.2$  °C. Mice were gently put onto the hot plate, recording the time of the mice licking their hind paws or jumping. A cut off latency of 60 s was used to avoid skin heat nociception. The latencies were recorded at 0 and 120 min after every NTG injection.

##### **Open field test (OFT)**

Mice were carefully placed into an open field chamber (40×40×30 cm) and allowed unrestricted freedom to

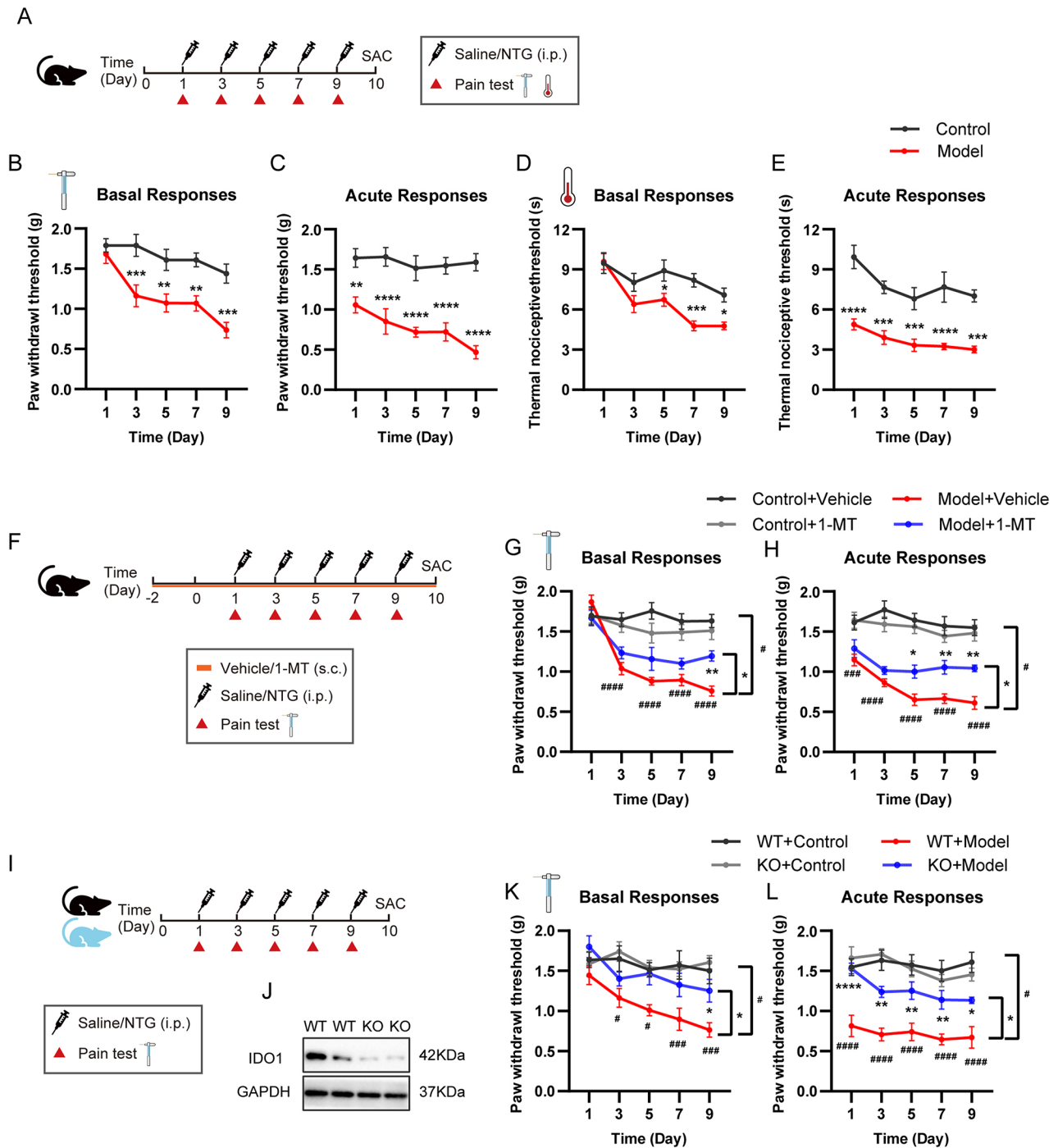


**Fig. 1** Inhibition of IDO1 alleviates hyperalgesia in the NTG-induced chronic migraine model. **(A)** Experimental timeline for inducing chronic migraine in mice with NTG and conducting pain behavioral tests (red triangle). **(B-C)** Basal and acute mechanical paw withdrawal thresholds measured by von Frey filament in response to mechanical stimuli ( $n=8$ ). **(D-E)** Basal and acute thermal nociceptive thresholds measured by paw withdrawal latency in response to thermal stimuli ( $n=8$ ). **(F)** Experimental timeline for treatment with 1-MT, an IDO1 inhibitor, in combination with NTG to assess its effects on pain sensitivity (red triangle). **(G-H)** Basal and acute mechanical paw withdrawal thresholds measured by von Frey filament in response to mechanical stimuli in vehicle and 1-MT injected mice ( $n=12$ ). **(I)** Experimental timeline for genetic knockout of IDO1 and NTG administration to evaluate the impact on pain sensitivity. **(J)** Western blotting analysis confirming IDO1 KO in mouse brain tissue compared to WT controls. GAPDH served as the loading control. **(K-L)** Basal and acute mechanical paw withdrawal thresholds measured by von Frey filament in response to mechanical stimuli in WT and IDO1 KO mice ( $n=8$ ). The data are shown as mean  $\pm$  SEM, \* or #  $p < 0.05$ , \*\*  $p < 0.01$ , \*\*\* or ###  $p < 0.001$ , \*\*\*\* or ####  $p < 0.0001$ ; two-way ANOVA in **(B-E, G, H, K, L)**

explore for 5 min. The central region constitutes a quarter of the chamber's base. SMART 3.0 software (Panlab, Spain) automatically calculated total distance and time spent in the central zone.

#### **Elevated plus maze test (EPM)**

The elevated-plus-maze apparatus consisted of two open arms (30×5 cm), two enclosed arms (30×5×15 cm), extending from a central platform (5×5 cm) elevated 50 cm above the ground. Mice were positioned on the central platform facing the same open arm, and allowed to explore for 5 min. SMART 3.0 software automatically calculated the time spent in the open and closed arms, as well as entries into open arms.

#### **Light aversion test**

The light-dark box consisted of two equal-size chambers (20×20×30 cm) connected by an opening (6×6 cm) in the middle, with a light (1000 lx) above the white chamber. Two hours after injection of NTG, mice were gently placed in the opening connection and allowed to explore for 30 min. The duration in light compartment was detected and calculated by the SMART 3.0 software.

#### **Sucrose preference test (SPT)**

Mice were habituated with two 1% sucrose solution identical water bottles for 24 h adaptation. Following that, mice were water and food deprived for 24 h and then received one bottle of water and one bottle of 1% sucrose solution, with bottle positions switched every 6 h. After 24 h, two bottles were taken and weighed to calculate the sucrose preference as  $[\text{sucrose water intake} / (\text{sucrose water intake} + \text{pure water intake})] \times 100\%$ .

#### **Forced swimming test (FST)**

The mice were placed in the glass cylinder (height 25 cm, diameter 10 cm) half-filled with water (22–24 °C) for 6 min and the duration of immobility was recorded during the final 4 min. The immobility was defined as floating without any movement except for those necessary for keeping the nose above the water. The cumulative immobility time was recorded manually (stop-watch) by an investigator who was blinded to the experimental groups.

#### **Stereotaxic virus injections**

Mice were anesthetized with pentobarbital sodium (75 mg/kg, i.p.) and positioned in a stereotaxic frame (RWD, China). Ophthalmic ointment was applied to avoid corneal drying. After shaving the head fur and disinfecting the skin, the skull surface was exposed with an incision. A 5 µL microsyringe (Gauge, China) was used to bilaterally deliver the virus particles into the ACC (from bregma: -1.2 mm anteroposterior, ±0.25 mm mediolateral and -2.00 mm dorsoventral) at a rate of 0.1 µL/min

under a microsyringe pump (Longer, China). The microsyringe remained in the injection place for 5–10 min and withdrawn slowly to prevent virus backflow. At the conclusion of the experiments, injection site accuracy within the targeted brain region was determined by the mCherry expressed by the AAV vectors, and mice with mistargeted injections were excluded from analysis before their data were unblinded.

The short hairpin RNA (shRNA) viruses and control virus were generated by Shanghai Sunbio Medical Biotechnology. A negative control (5'-GGACATCACCTCC CACAACGAG-3'), shRNA1 (5'-GAACTGGAGGCACT GATTTAA-3'), shRNA2 (5'-GGATGCATCACCATGG CATAT-3') or shRNA3 (5'-CGTAAGGTCTTGCCAAG AAAT-3') with a CTCGAG hairpin loop and TTTTTT termination sequence were generated, annealed, and cloned into a pAAV-CAG-mCherry entry vector.

#### **Fiber photometry recording**

Mice were unilaterally infected with AAV2/9-CaMKII $\alpha$ -GCaMP6m into ACC and implanted an optical fiber into the same site. Two weeks later, the GCaMP6m fluorescence signals were detected using a fiber photometry system (ThinkerTech, China) with a 488-nm laser power (10–15 µW) during the mechanical pain threshold test. For recording the responses of ACC neurons during von Frey test, the filament stimulation (1.0 g) was delivered onto the hind paw for ten times before and 2 h after NTG administration, depending on there was a positive response. The inter-trial interval randomly varied between 2 and 4 min. The simultaneous recording of neuronal Ca<sup>2+</sup> signals and behavior videos was conducted. The values of Ca<sup>2+</sup> signal changes ( $\Delta F/F$  (%)) were calculated as  $(F - F_0)/F_0 \times 100\%$ , where F<sub>0</sub> was the averaged baseline fluorescence signal recorded 10 s before stimuli, analyzed with MATLAB.

#### **Slice Preparation and electrophysiological recordings**

Patch-clamp recordings in brain slices were prepared according to the procedures described previously [34, 35]. Mice were subjected to deep anesthesia with pentobarbital sodium (75 mg/kg, i.p.) and then intracardially perfused with ice-cold, oxygenated (95% O<sub>2</sub> and 5% CO<sub>2</sub>) modified sucrose-slicing artificial cerebrospinal fluid (ACSF) composed of the following (in mM): 220 sucrose, 26 NaHCO<sub>3</sub>, 10 D-glucose, 2 KCl, 12 MgSO<sub>4</sub>, 1.3 NaH<sub>2</sub>PO<sub>4</sub> and 0.2 CaCl<sub>2</sub>. The mice were sacrificed by decapitation, and their brains were promptly extracted and chilled by immersion in oxygenated sucrose-slicing ACSF. Coronal slices (300 µm thick) encompassing the ACC were prepared using a vibratome (Leica, VT1000S). The slices were then allowed to recover for at least 30 min in a holding chamber filled with continuously oxygenated ACSF (recording ACSF) consisting of the following

(in mM): 124 NaCl, 3 KCl, 26 NaHCO<sub>3</sub>, 10 D-glucose, 1 MgSO<sub>4</sub>, 1.25 NaH<sub>2</sub>PO<sub>4</sub>, and 2 CaCl<sub>2</sub>, at pH 7.4, 305 mOsm, and maintained at a temperature of 34 °C, followed by an additional incubation period of at least 1 h at room temperature until required. For electrophysiological recording, slices were transferred to the recording chamber, which was continuously perfused with oxygenated ACSF at a rate of 2–3 mL/min. Whole-cell patch clamp recordings were performed by using an upright microscope (Nikon, ECLIPSE FN1) equipped with a 40× water-immersion lens and an infrared-sensitive camera (DAGE-MTI, IR-1000E). Patch pipettes were fabricated from filamented borosilicate glass capillary tubes (inner diameter, 0.84 μm) by using a horizontal puller (Sutter Instruments, P-97). Recordings were acquired employing a multiclamp 700B amplifier and pClamp software (Molecular Devices). The data were low-pass filtered at 1 kHz and sampled at 10 kHz with a Digidata 1440 A device (Molecular Devices).

To assess spontaneous excitatory postsynaptic currents (sEPSCs) and spontaneous inhibitory postsynaptic currents (sIPSCs) from the same neurons, recordings were conducted in voltage-clamp mode while maintaining the membrane potential either at the reversal potential for GABA<sub>A</sub> receptor-mediated EPSCs (-60 mV) or at the reversal potential for ionotropic glutamate receptors-mediated IPSCs (0 mV). The pipette resistance was typically 6–8 MΩ after being filled with an internal solution (in mM): 110 Cs<sub>2</sub>SO<sub>4</sub>, 0.5 CaCl<sub>2</sub>, 2 MgCl<sub>2</sub>, 5 EGTA, 5 HEPES, 5 TEA, and 5 Mg-ATP (pH 7.3, 285 mOsm). The intrinsic membrane properties, encompassing resting membrane potential (RMP), input resistance (R<sub>in</sub>), rheobase (minimal current required to induce neuronal firing), action potential (AP) threshold, and the firing number (APs induced by injecting sequentially increasing current steps) were recorded in current-clamp mode using an internal recording solution containing (in mM): 130 K-gluconate, 20 KCl, 10 HEPES, 0.2 EGTA, 4 Mg-ATP, 0.3 Na-GTP, and 10 NaCreatine, with a pH of 7.3 and osmolality of 285 mOsm. For each cell, the recordings were commenced after stabilization of the holding potential approximately 2–5 min after the break-in. Only the cells with a series resistance < 30 MΩ and leak currents < 100 pA were considered for further analysis. The synaptic currents were recorded in the voltage-clamp mode and analyzed with the Mini analysis (Synaptosoft Inc.) and Clampfit 10.7 (Molecular Devices).

#### RNA sequencing

To isolate cells for bulk RNA-seq, mice were euthanized, and the ACC area was punched out and subjected to RNA isolation for RNA sequencing analysis. cDNA library construction and sequencing were performed by Azenta Life Sciences company (Suzhou, China). The

library preparations were sequenced on Illumina Nova-seq platform, and 2×150-bp paired-end reads were generated. The index of the reference genome was built using Hisat2, and paired-end clean reads were aligned to the reference genome using Hisat2 (v2.2.1). HTSeq v0.6.1 was used to count the number of reads that mapped to each gene. The expression of each gene in FPKM was calculated based on the length of the gene and the number of reads that mapped to this gene by dealing with R language. We identified differentially expressed genes (DEGs) between samples and performed clustering analysis and functional annotation. Genes with |FoldChange| > 1.5 and an adjusted P-value < 0.05 found by DESeq2 were assigned as DEGs. Pathways enriched in the DEGs were annotated with the Gene Ontology (GO), The Kyoto Encyclopedia of Genes and Genomes (KEGG) pathway, and Gene Set Enrichment Analysis (GSEA) database.

#### Western blotting

Bilateral ACC tissue was acquired from 300 μm thick sections by using a vibratome. The tissue was homogenized in ice-cold RIPA buffer (50 mM Tris, 150 mM NaCl, 1% TritonX-100, 1% sodium deoxycholate, 0.1% SDS, pH 7.4) containing 0.5% protease and phosphatase inhibitors cocktail (Beyotime, P1045). The samples were lysed on ice for 30 min and then centrifuged at 12,000 rpm at 4 °C for 15 min. Protein concentrations were determined with BCA Protein Assay Kit (Beyotime, P0012), then combined with 5× SDS loading buffer and heated up to 100 °C for 10 min. Extracted proteins were separated by SDS-PAGE in 10% gels and transferred them onto PVDF membranes (Millipore, 0.45 μm). After blocking with 5% nonfat milk at room temperature for 2 h, the membranes were incubated overnight at 4 °C with primary antibodies: IDO1 (1:1000, rat, Santa Cruz, sc-53978), IFN-γ (1:1000, rabbit, Affinity Biosciences, DF6045), IFN-β (1:1000, rabbit, Affinity Biosciences, DF6471), GAPDH (1:50000, mouse, Proteintech, 60004-1-Ig). The membranes were washed three times for 10 min each with TBST and incubated with HRP-conjugated secondary antibody (1:50000, anti-mouse IgG-HRP, Proteintech, SA00001-1; 1:50000, anti-rabbit IgG-HRP, Proteintech, SA00001-2; 1:30000, anti-Rat IgG-HRP, Proteintech, SA00001-15) for 2 h at room temperature. Protein bands were visualized using Image Lab software (ChemiDoc XRS+, Bio-Rad, USA) and quantified using ImageJ software.

#### Immunofluorescence staining

Mice anesthetized with pentobarbital sodium (75 mg/kg, i.p.) were intracardially perfused with ice-cold PBS followed by 4% paraformaldehyde (PFA) solution. The extracted brains were post-fixed in 4% PFA at 4 °C overnight, and then dehydrated with 30% sucrose in PBS at 4 °C for at least 48 h. Frozen brains were cut into

coronal slices (40  $\mu\text{m}$ ) using a microtome cryostat (Leica CM3050 S). The ACC brain slices were rinsed with PBS three times for 10 min each time, followed by exposure to citrate buffer (10 mM sodium citrate buffer, pH = 6.0) for 30 min at 80 °C. After cooling to room temperature, brain slices were washed three times with PBS for 10 min and incubated with blocking solution (5% Bovine serum albumin, 1% Triton X-100 in PBS) at room temperature for 1 h. Sections were then incubated overnight at 4 °C in primary antibodies diluted with 5% BSA, including c-Fos (1:500, rabbit, Millipore, ABE457), IBA1 (1:500, rat, Synaptic Systems, 234 017), IDO1 (1:500, rabbit, Proteintech, 13268-1-AP), Synapsin1 (Syn1) (1:500, rabbit, Cell Signaling Technology, #5297), postsynaptic density protein 95 (PSD95) (1:500, rabbit, Invitrogen, 51-6900). After that, the slices were washed three times with PBS for 10 min each, and incubated with Alexa 488- or 594-conjugated secondary antibodies (1:500, Yeasen) for 2 h at room temperature in a light-resistant containers. Slices were then stained with DAPI (1  $\mu\text{L}/\text{mL}$ , Sigma-Aldrich, D9542) for 10 min and washed three times with PBS for 10 min each, mounted and coverslipped with antifade solution, and stored at 4 °C away from light. Images were captured using a confocal laser-scanning microscope (Olympus FV3000, Japan).

### Three-dimensional (3D) reconstruction

High-resolution confocal images were performed on an Olympus FV3000 microscope using a 60 $\times$ /1.42 NA oil-immersion lens, with 1  $\mu\text{m}$  intervals in the z-stack. Images were reconstructed using Imaris 9.0.0 software (Bitplane). The total process length and Sholl analysis of each microglia were quantified with “Filaments” function. For microglia engulfment analysis, the number of Syn1<sup>+</sup> and PSD95<sup>+</sup> puncta within IBA1<sup>+</sup> microglia were assessed and synaptic marker puncta were reconstructed using “Spots” function [36].

### Statistical analysis

No statistical methods were used to predetermine the sample size in experiments. Statistical analysis and graphing were conducted using GraphPad Prism (version 8.0) software. All results are expressed as the mean  $\pm$  standard error (SEM). Prior to statistical comparison analysis, all data were tested for normal distribution and homogeneity of variance (Shapiro-Wilk test, Levene test). The unpaired two-tailed Student's t test was used for comparisons between two groups. One-way ANOVA or two-way ANOVA followed by Bonferroni or Dunnett post hoc test was used for analyses with multiple comparisons. For non-normally distributed data, Mann-Whitney U test or Kruskal-Wallis test was applied. A value of  $P < 0.05$  was considered to be statistically significant.

## Results

### Inhibition of IDO1 alleviates hyperalgesia in the NTG-induced chronic migraine model

For a first-order validation experiment, we established a chronic migraine mouse model through intermittent intraperitoneal injections of NTG, and assessed mechanical and thermal sensitivity using the von Frey and hot-plate tests, respectively (Fig. 1A). While no significant differences were observed in the basal mechanical and thermal nociceptive thresholds between groups on day 1, chronic NTG-induction resulted in a gradually decreased in both basal and acute responses (Fig. 1B-E). As photophobia is one of the most common symptoms of migraine [1], we utilized the light-dark transition to assess light aversion behavior. Compared with control mice, NTG-treated mice spent significantly less time in the light chamber (Supplementary Fig. 1). These results indicate that the NTG-induced chronic migraine model effectively mimics the hyperalgesia and photophobia characteristic of migraine.

To elucidate the role of IDO1 in chronic migraine, we inactivated IDO1 with its inhibitor 1-MT (Fig. 1F), and found that treatment with 1-MT significantly attenuated the paw mechanical pain thresholds in chronic migraine mice, without affecting those in the control group (Fig. 1G-H). To further evaluate the physiological significance of IDO1 function, we employed IDO1 KO mice (Fig. 1I-J and Supplementary Fig. 2). Consistent with our pharmacological results, genetic deletion of IDO1 led to an increase paw mechanical pain threshold compared with that in the WT + Model group (Fig. 1K-L). Collectively, these data suggest that pharmacological inhibition and genetic deletion of IDO1 alleviate pain hypersensitivity in the NTG-induced chronic migraine model.

### ACC neuronal activity is enhanced in chronic migraine model mice

To identify the brain regions responsive to chronic migraine, we examined the expression of c-Fos, a well-established maker of neuronal activity, by quantifying positive cells in regions relevant to pain modulation and emotional-affective dimension of pain [37]. The ACC showed a significant increase in the relative expression of c-Fos<sup>+</sup> cells (Fig. 2A, B). To monitor ACC pyramidal neuronal activity under freely moving conditions, we injected AAV-CaMKII $\alpha$ -GCaMP6m and implanted an optical fiber targeting ACC, as well as measured compound Ca<sup>2+</sup> activity in real-time using fiber photometry technique (Fig. 2C, D). There was an increase in Ca<sup>2+</sup> signaling in the ACC in response to von Frey filament stimuli in the NTG-treated mice, whereas no such response was detected in the mice prior to NTG injection (Fig. 2E-H).

Considering the activity changes observed in c-Fos and fiber photometry experiments could result from altered

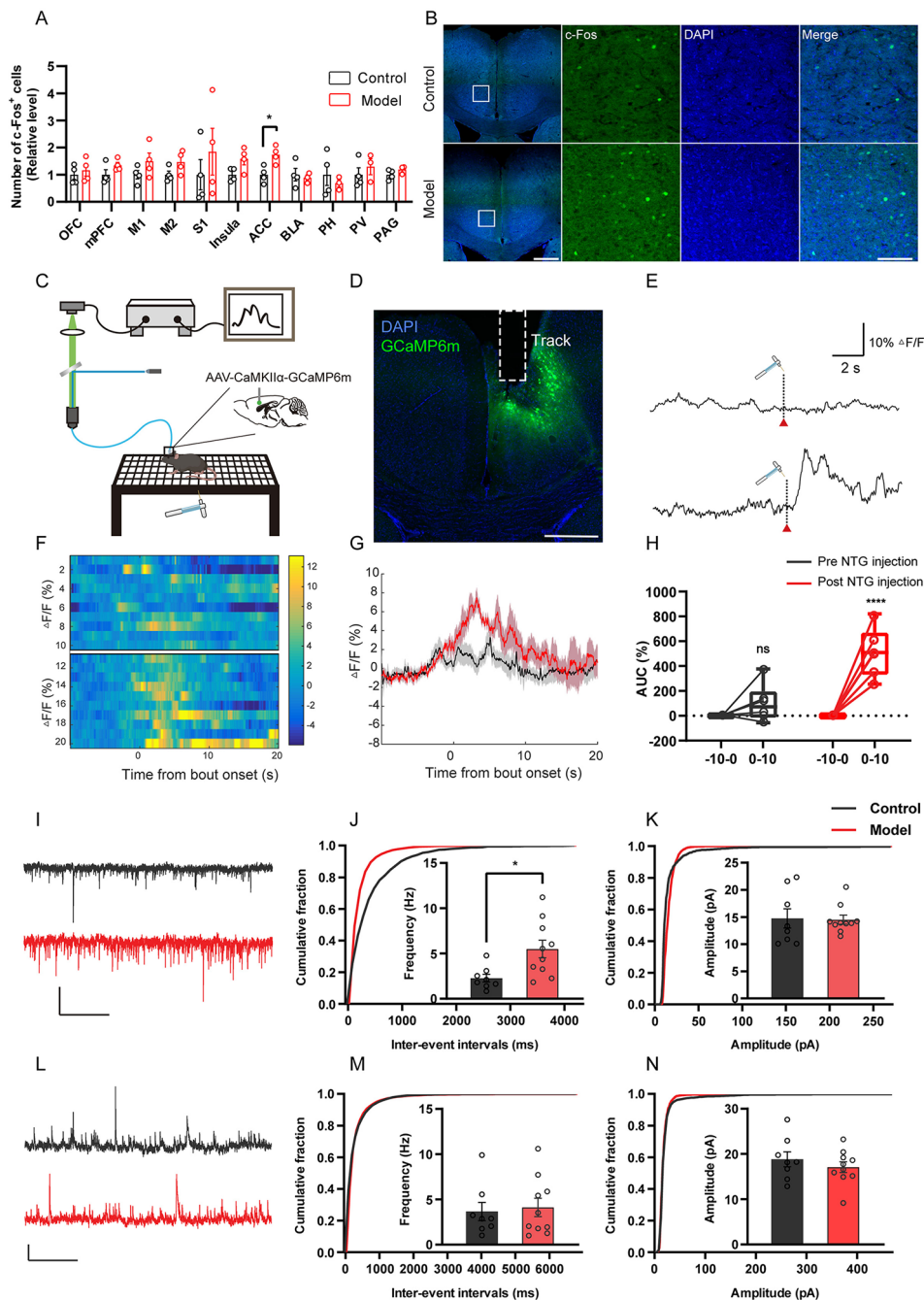


**Fig. 2** Enhanced ACC neuronal activity contributes to pain hypersensitivity. **(A)** Quantification of c-Fos<sup>+</sup> cells in different brain regions of saline- and NTG-treated mice ( $n=4$ ). **(B)** Representative images of c-Fos immunofluorescence staining in the ACC. Scale bar (left), 500  $\mu\text{m}$ ; Scale bar (right), 100  $\mu\text{m}$ . **(C)** Schematic diagram of the fiber photometry recording. **(D)** Representative image verifying the expression of GCaMP6m in optical fiber bundle above the ACC. Scale bar, 500  $\mu\text{m}$ . **(E)** Example raw traces showing the GCaMP6m fluorescence levels in response to von Frey filament stimuli in mice before NTG injection (upper line) and 2 h after injection (bottom line). Scale bar, 10%  $\Delta\text{F}/\text{F}$ , 2 s. **(F-G)** Representative heatmaps and traces of fluorescence aligned to stimuli pre- and post-NTG injection. **(H)** Graphic representation of **(C)** for responses to von Frey filament stimuli pre- and post-NTG injection ( $n=6$ ). **(I)** Example traces of 10 s recordings of sEPSCs from ACC neurons in WT mice, as indicated. Scale bars, 20 pA, 2 s. **(J-K)** Cumulative probability plots of sEPSC inter-event interval and amplitude, with additional summary graphs demonstrating the frequency and amplitude of sEPSCs recorded from ACC neurons in WT mice, respectively ( $n=8-10$  cells from 4 to 5 mice). **(L)** Example traces of 10 s recordings of sIPSCs from ACC neurons in WT mice, as indicated. Scale bars, 20 pA, 2 s. **(M-N)** Cumulative probability plots of sIPSC inter-event interval and amplitude, with additional summary graphs demonstrating the frequency and amplitude of sIPSCs recorded from ACC neurons in WT mice, respectively ( $n=8-10$  cells from 4 to 5 mice). The data are shown as mean  $\pm$  SEM, \* $p < 0.05$ , \*\*\*\* $p < 0.0001$ ; Student's  $t$  test in **(A, J, N)**, Mann-Whitney U test in **(K, M)**, two-way ANOVA in **(H)**

synaptic transmission or intrinsic membrane properties, we employed whole-cell patch-clamp electrophysiological recordings. To assess the E/I balance, we recorded sEPSC and sIPSC in the ACC of NTG-treated mice. The sEPSC frequency was significantly increased, whereas the sEPSC amplitude, sIPSC frequency and amplitude were not changed in the model mice, resulting in an overturn of the E/I balance (Fig. 2I-N and Supplementary Fig. 3A, B). Additionally, there were no differences in AP firing frequency, RMP,  $R_{in}$ , rheobase and AP threshold potential in the ACC between the two groups (Supplementary Fig. 3C-H).

These results suggest that the enhancement of ACC neuronal activity following NTG-induced chronic migraine is due to an increase in the E/I balance rather than changes in intrinsic membrane properties.

### **IDO1 in the ACC regulates pain hypersensitivity in chronic migraine**

Our previous results indicate a role for IDO1 in chronic migraine and suggest that the ACC is a key brain region involved, raising the possibility that IDO1 in the ACC may also regulate migraine-associated pain. We examined IDO1 expression in the ACC of chronic migraine model mice via western blotting (Fig. 3A). Our results revealed a significant increase in IDO1 protein expression in the ACC of NTG-treated mice compared with saline-treated controls (Fig. 3B, C). Similar results were observed in other chronic migraine models, including CSD, ES- and reserpine-induced models (Supplementary Fig. 4D-F).

To further investigate the role of ACC IDO1 in chronic migraine, we used AAV-shRNA to knockdown IDO1 expression in chronic migraine mice. We first injected AAV-CAG-shRNA-mCherry or control AAV-CAG-mCherry into the ACC (Fig. 3D-E). Western blotting confirmed the knockdown efficiency, showing significant reductions in IDO1 protein expression with shRNA1 and shRNA2 compared with the mCherry control (Fig. 3F-G). AAV-CAG-shRNA1-mCherry, which has a relatively high titer and in vivo transduction efficiency, was selected for subsequent experiments. Our results showed that knockdown of IDO1 in the ACC alleviated mechanical pain hypersensitivity in chronic migraine model mice, whereas it had no effect on pain thresholds in mCherry mice (Fig. 3H-J).

To determine whether changes in IDO1 levels affect synaptic function, we performed whole-cell patch-clamp recordings in the ACC. Our data indicated that the frequency and amplitude of the sEPSC remained unchanged in the KO mice after saline injection. In NTG-treated WT mice, the sEPSC frequency significantly increased, but this increase was reversed by IDO1 deletion (Fig. 3K-M). The frequency and amplitude of the sIPSC were not

altered in either WT or KO mice after saline or NTG injection (Fig. 3N-P). Consequently, The E/I frequency ratio and amplitude ratio presented no significant differences between WT and KO mice treated with or without NTG (Supplementary Fig. 5A-B).

### **IDO1 deletion alleviates microglial activation and microglia-mediated synaptic pruning in chronic migraine**

Microglia, the resident immune cells of the central nervous system, act as the primary mediators of neuroinflammation [38]. Our previous research revealed a link between IDO1 and inflammation [22], together with our current findings of elevated IDO1 expression in a chronic migraine mouse model, suggesting a potential connection between IDO1 and microglial activity in chronic migraine. Immunofluorescence staining for IBA1, a recognized microglial marker, was conducted to examine IDO1 colocalization within microglia. We observed coexpression of IDO1 (red) and IBA1 (green) in microglia, with increased numbers of IDO1<sup>+</sup> and IBA1<sup>+</sup> coexpressing cells in NTG-treated mice (Fig. 4A, B). Moreover, the number of microglia in the ACC was greater in NTG-treated WT mice than in that of saline-treated WT mice, with no differences observed in KO mice regardless of treatment (Fig. 4C, D). Importantly, NTG-treated KO mice exhibited significantly fewer microglia compared to NTG-treated WT mice (Fig. 4C, D).

Morphometric analyses of individual microglia, on the basis of 3D reconstructions, quantitatively revealed alterations in the structure of microglia during chronic migraine. Semiautomatic quantitative 3D morphometric measurements of microglia revealed significantly shorter and less complex processes in NTG-treated WT mice than in both saline-treated WT mice and NTG-treated KO mice (Fig. 4E-G). In contrast, the total process length and complexity in KO mice were still intact after injection of saline or NTG (Fig. 4E-G). These results indicate that microglial reactivity in the ACC is increased in response to NTG stimulation.

Microglia participate in synaptic pruning, and dysregulated pruning is associated with various brain diseases [39, 40]. To investigate the potential link between microglia and neuronal synaptic pruning in chronic migraine, we assessed the colocalization of synaptic protein markers, such as the presynaptic marker Syn1 or the postsynaptic marker PSD95, with IBA1-labeled microglia in the ACC. Abundant immunoreactive puncta (red) of Syn1 colocalized with IBA1-labeled microglia (gray) in the ACC of NTG-treated WT mice, but not in those of saline-treated WT mice. Syn1 engulfment by microglia was significantly decreased in NTG-treated KO mice compared with NTG-treated WT mice (Fig. 4H, I). No significant changes in PSD95 (red) engulfment by microglia

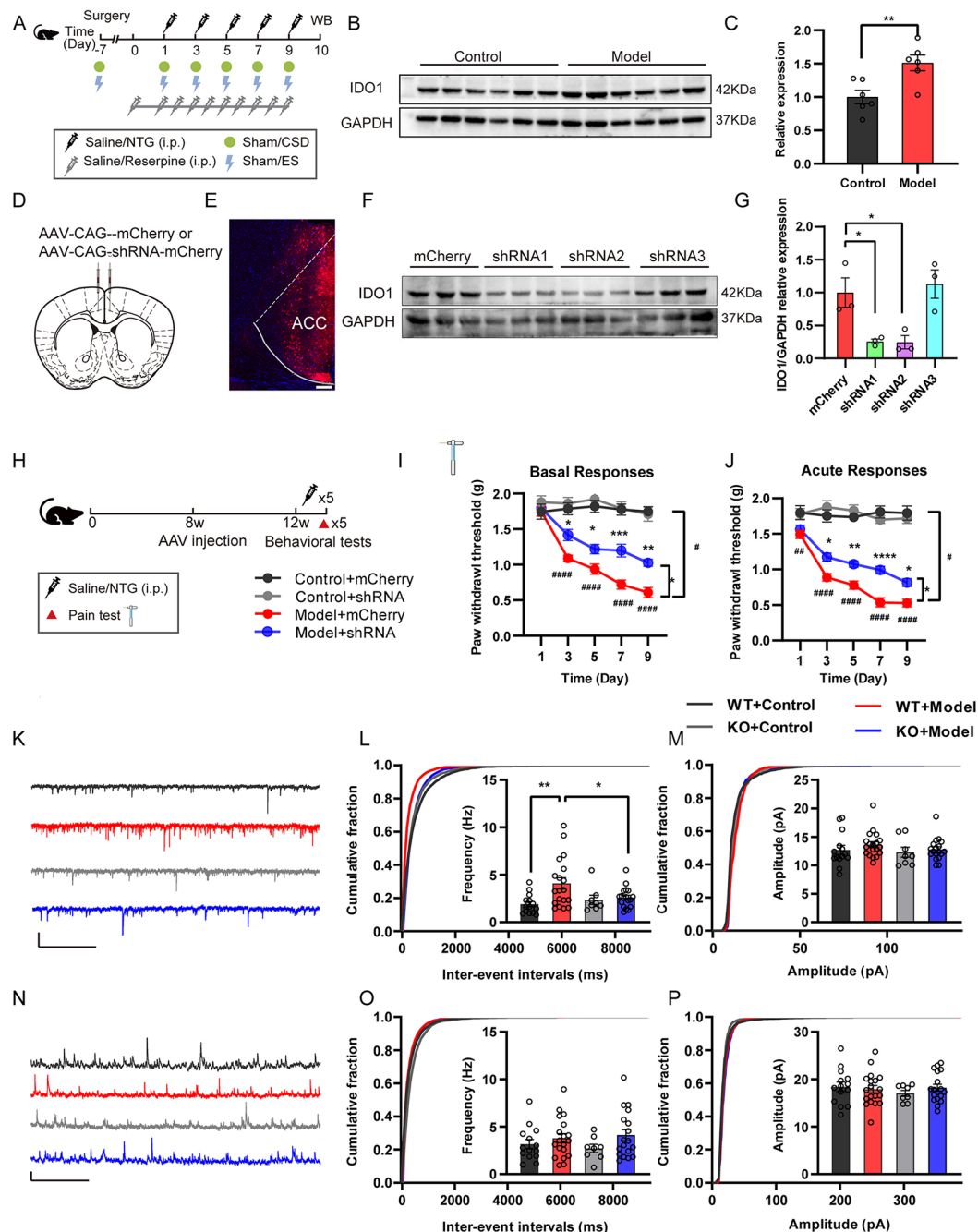


**Fig. 3** IDO1 in the ACC regulates pain hypersensitivity in chronic migraine mice. **(A)** Procedure for evaluation of IDO1 protein expression in various chronic mouse models of migraine using western blotting. **(B)** Increased IDO1 protein levels in the ACC of NTG-treated mice. **(C)** Quantitative analysis of the data in **(B)**. The IDO1 band density was normalized to the loading control GAPDH ( $n=6$ ). **(D-E)** Schematic of viral injection, and representative image of viral injection site in the ACC. Scale bar, 200  $\mu\text{m}$ . **(F)** The silencing effects of three IDO1 shRNAs targeted to different sequences, analyzed with western blotting. **(G)** Quantitative analysis of the data in **(F)**. The IDO1 band density was normalized to control GAPDH (AAV-CAG-mCherry) ( $n=3$ ). **(H)** Schematic of the experiment used to evaluate pain sensitivity in WT mice injected with AAVs. **(I-J)** Basal and acute mechanical paw withdrawal thresholds measured by von Frey filament in response to mechanical stimuli in WT mice treated with mCherry and shRNA ( $n=12$ ). **(K)** Example traces of 10 s recordings of sEPSCs from ACC neurons among groups, as indicated. Scale bars, 20 pA, 2 s. **(L-M)** Cumulative probability plots of sEPSC inter-event interval and amplitude, with additional summary graphs demonstrating the frequency and amplitude of sEPSCs recorded from ACC neurons among groups ( $n=8-19$  cells from 4-5 mice). **(N)** Example traces of 10 s recordings of sIPSCs from ACC neurons among groups, as indicated. Scale bars, 20 pA, 2 s. **(O-P)** Cumulative probability plots of sIPSC inter-event interval and amplitude, with additional summary graphs demonstrating the frequency and amplitude of sIPSCs recorded from ACC neurons among groups ( $n=8-19$  cells from 4-5 mice). The data are shown as mean  $\pm$  SEM, \* $p < 0.05$ , \*\* $p < 0.01$ , \*\*\* $p < 0.001$ , \*\*\*\* or ##### $p < 0.0001$ ; Student's t test in **(C)**, one-way ANOVA in **(G, L, M, O, P)**, two-way ANOVA in **(I, J)**

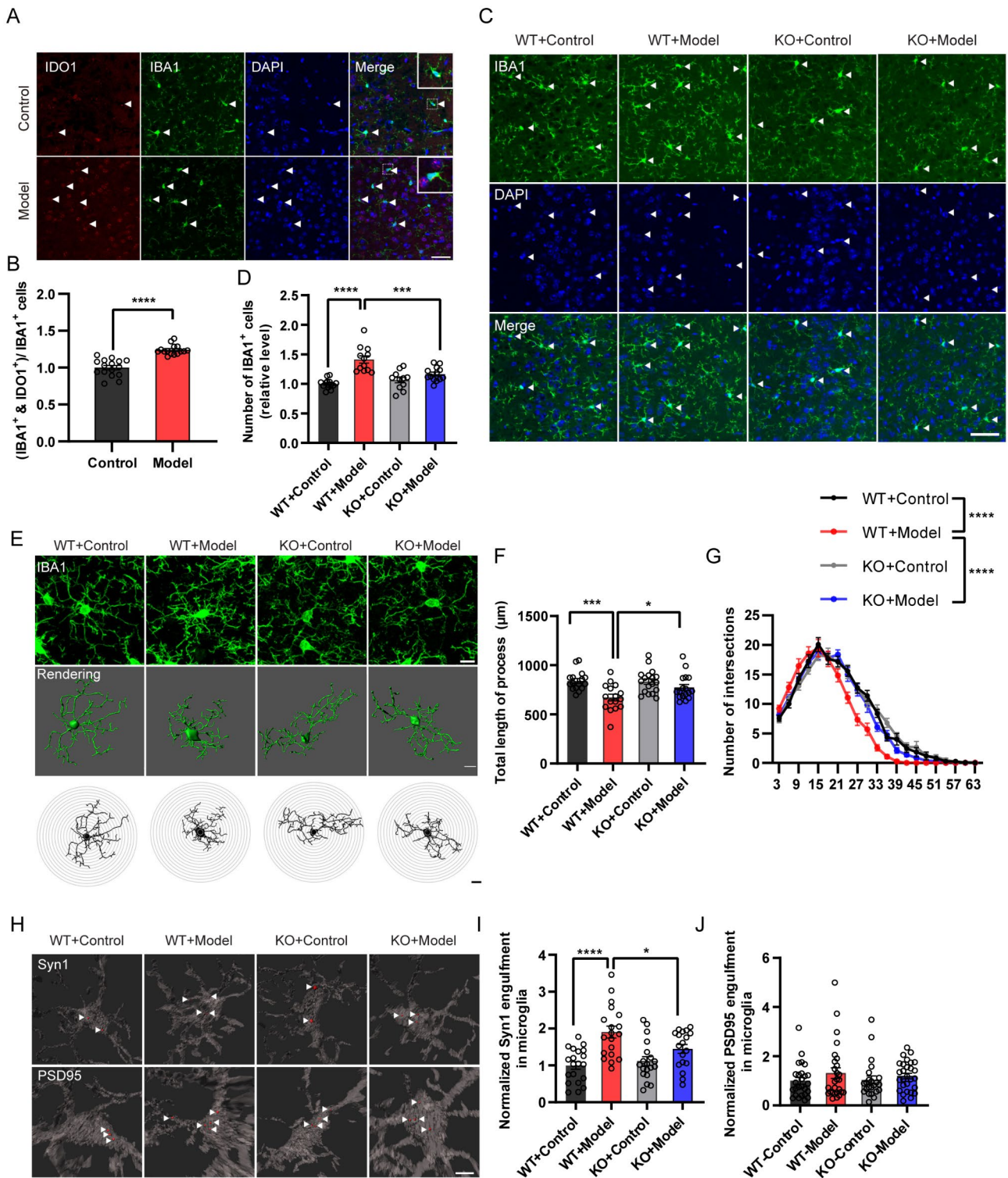


**Fig. 4** (See legend on next page.)

(See figure on previous page.)

**Fig. 4** Knockout of IDO1 ameliorates IBA1+ cells-mediated engulfment of synapse in chronic migraine mice. (A) Representative immunofluorescence images showing colocalization of IDO1 and IBA1 in the ACC of saline- or NTG-treated mice. Scale bars, 20  $\mu\text{m}$ . (B) Quantification of colocalization between IDO1+ and IBA1+ cell numbers in the ACC from saline- and NTG-treated mice ( $n = 15\text{--}16$  slices from 4 mice). (C) Representative images of IBA1 immunostaining in the ACC of saline- or NTG-treated mice. Scale bars, 50  $\mu\text{m}$ . (D) Quantification of IBA1+ cells in the ACC of WT and KO mice 2 h after saline or NTG administration ( $n = 11\text{--}14$  slices from 4 mice). (E) Representative 3D reconstruction images and Sholl analysis of microglia in the ACC of WT and KO mice with or without NTG-treated. Scale bars, 10  $\mu\text{m}$  (zoom) and 5  $\mu\text{m}$  (rendering). (F) Imaris-based quantification of cell morphometry and total process length of IBA1+ microglia in the ACC from saline- and NTG-treated mice ( $n = 16\text{--}18$  slices from 4 mice). (G) Sholl analysis of microglial morphology in saline- or NTG-treated mice ( $n = 16\text{--}18$  slices from 4 mice). (H) Representative images and 3D surface rendering of IBA1+ microglia (gray) containing Syn1+ and PSD95+ (red) in the ACC from saline- and NTG-treated mice. Scale bars, 2  $\mu\text{m}$ . (I) Quantification of Syn1+ punta in microglia in mice as indicated in (H) ( $n = 18\text{--}20$  cells from 4 mice). (J) Quantification of PSD95+ punta in microglia in mice as indicated in (H) ( $n = 18\text{--}20$  cells from 4 mice). The data are shown as mean  $\pm$  SEM, \* $p < 0.05$ , \*\*\* $p < 0.001$ , \*\*\*\* $p < 0.0001$ ; Student's t test in (B), one-way ANOVA in (D, F, I, J), two-way ANOVA in (G)

(gray) were detected between NTG- and saline-treated mice (Fig. 4H, J).

Collectively, these results reveal that IDO1 regulates microglial activation and synaptic pruning in chronic migraine, providing insights into the mechanisms underlying neuroinflammation and pain hypersensitivity.

#### IDO1 regulates chronic migraine through the IFN signaling pathway

To investigate the underlying mechanism by which IDO1 regulates chronic migraine, we performed RNA sequencing on ACC tissues from both WT and KO chronic migraine mice. Principal component analysis (PCA) showed a clear separation between saline- and NTG-treated mice, with NTG-treated KO mice closely aligning with, but still differing slightly from, NTG-treated WT mice (Fig. 5A). Volcano plots indicated significant changes in gene expression: 367 genes were upregulated and 223 genes were downregulated in NTG-treated WT mice compared with saline-treated controls (Fig. 5B); 261 genes were upregulated and 374 genes were downregulated in NTG-treated KO mice compared with saline-treated controls (Fig. 5C); and 142 genes were upregulated and 256 genes were downregulated in NTG-treated KO mice compared with NTG-treated WT mice (Fig. 5D). Venn diagrams identified 430 DEGs unique to NTG-treated WT mice but not altered in NTG-treated KO mice (Fig. 5E). A heatmap was generated to visualize the expression profiles of these DEGs across the four groups (Fig. 5F). GO, KEGG pathway, and GSEA analyses implicated these DEGs as predominantly associated with the IFN signaling pathway, including type I and type II interferons (Fig. 5G–J).

The IFN family has been implicated as a key regulatory molecule in the inflammatory response [41]. Western blotting analysis revealed significantly elevated IFN- $\gamma$  expression in the ACC of NTG-treated WT mice compared with both saline-treated WT mice and NTG-treated KO mice (Fig. 5K, L). No significant changes were observed in IFN- $\beta$  expression among these mice (Fig. 5M, N). To directly assess the involvement of the IFN signaling pathway in IDO1-mediated pain sensitization, we employed pharmacological intervention

(Fig. 5O). Tilorone dihydrochloride, an IFN agonist, attenuated mechanical pain thresholds in shRNA-treated mice following NTG injection, effectively reversing the rescue effect of IDO1 knockdown (Fig. 5P, Q). These results indicate that IDO1 modulates pain sensitization and microglia-mediated neuroinflammation through the IFN signaling pathway in chronic migraine.

#### IDO1 in the ACC modulates anxiety-like behaviors associated with chronic migraine

Anxiety and mood disorders are prominent psychiatric comorbidities associated with chronic migraine. Given the role of the ACC in pain processing and its critical involvement in negative emotional disorders associated with chronic pain [42, 43], we investigated anxiety- and depressive-like behaviors induced by chronic migraine. We found that NTG-treated mice displayed anxiety-like behaviors in OFT and EPM behavioral assays, with reduced center-zone time and total distance in the OFT (Fig. 6A–C), as well as reduced open-arm time, increased closed-arm time, and fewer open-arm entries in the EPM (Fig. 6D–G). However, depressive-like behaviors were not observed in NTG-treated mice, as assessed by the SPT and FST (Supplementary Fig. 6). These results confirm that NTG-induced chronic migraine is comorbid with anxiety.

To further investigate the role of ACC IDO1 in migraine-related anxiety-like behaviors, we utilized AAV-mediated knockdown of IDO1. As expected, there were no significant differences in general locomotor activity assessed by the OFT or anxiety-like behavior assessed by the EPM (Supplementary Fig. 7). Compared with saline-treated control mice, NTG-treated mCherry mice consistently presented significantly shorter center-zone times and locomotor activity. However, these anxiety-like behaviors in the OFT were not rescued in NTG-treated shRNA-treated mice (Fig. 6H–J). Compared with NTG-treated mCherry mice, NTG-treated shRNA-treated mice presented significantly increased open-arm time and decreased closed-arm time in the EPM test, although the number of open-arm entries was not significantly rescued (Fig. 6K–N). These results suggest that ACC IDO1 participates in chronic migraine-induced anxiety-like

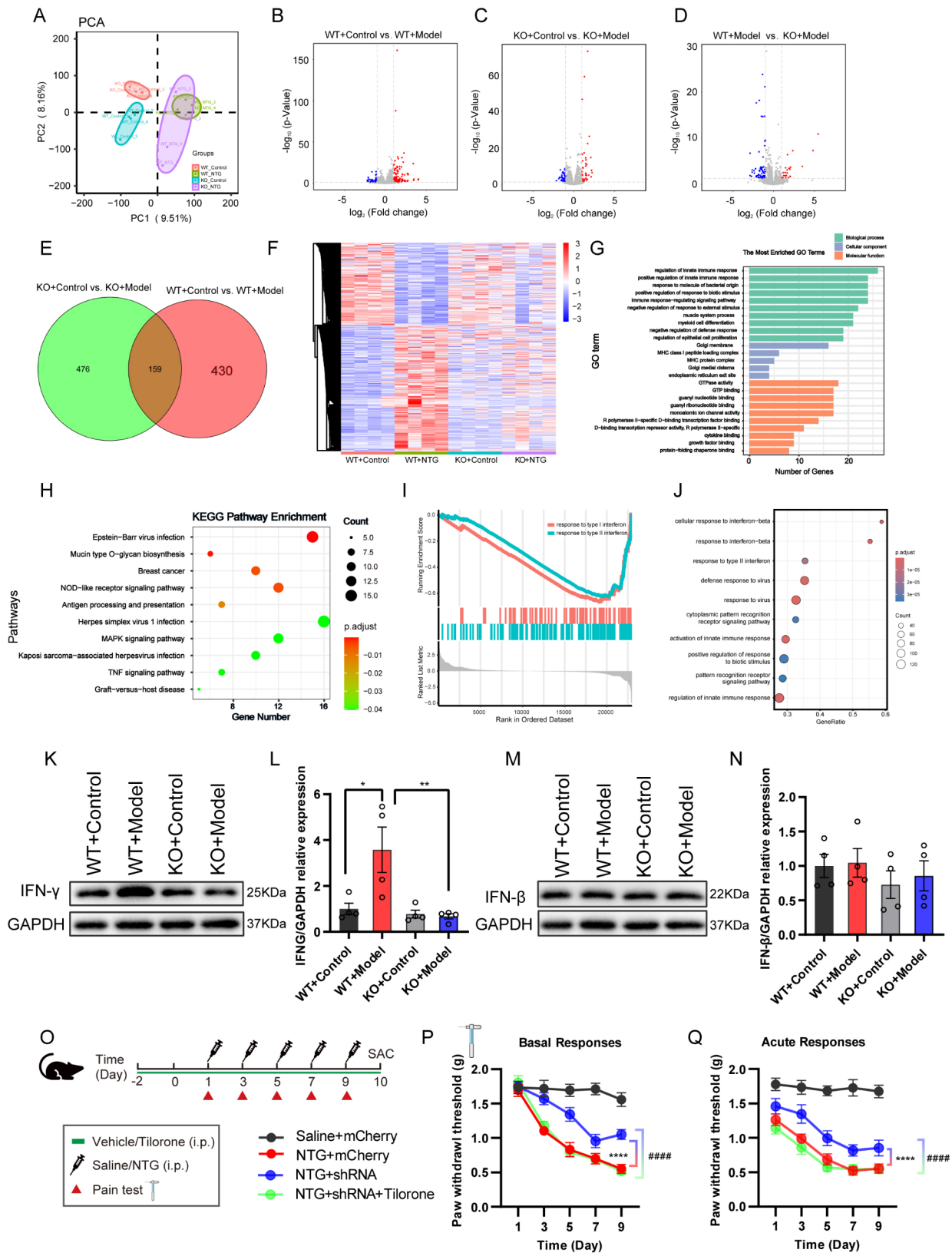


Fig. 5 (See legend on next page.)

(See figure on previous page.)

**Fig. 5** IDO1 regulates pain sensitivity through IFN signaling pathway in chronic migraine. **(A)** PCA plot indicating distinct clustering of gene expression profiles in the ACC of WT and IDO1 KO mice treated with saline or NTG ( $n=4$ ). **(B–D)** Volcano plots illustrating differentially expressed genes (DEGs) in the ACC: (B) WT + Control vs. WT + Model, (C) KO + Control vs. KO + Model, (D) WT + Model vs. KO + Model ( $n=4$ ). **(E)** Venn diagrams depicting the overlap of DEGs between WT + Control vs. WT + Model and KO + Control vs. KO + Model groups, identifying 430 DEGs unique to NTG-treated WT mice but not altered in NTG-treated KO mice. **(F)** Heatmap representing the expression levels of the 430 unique DEGs in the ACC across all experimental groups, indicating distinct expression patterns. **(G–H)** GO and KEGG were used for functional enrichment analysis of the 430 unique DEGs. **(I)** GSEA plot for the IFN signaling pathway. **(J)** Enrichment plots for the top 10 pathways by GSEA. **(K)** Increased IFN- $\gamma$  protein expression in the ACC of NTG-treated WT mice. **(L)** Quantitative analysis of the data in **(K)**. The IFN- $\gamma$  band density was normalized to the loading control GAPDH ( $n=4$ ). **(M)** No changes of IFN- $\beta$  between NTG- or saline-treated mice. **(N)** Quantitative analysis of the data in **(M)**. The IFN- $\beta$  band density was normalized to the loading control GAPDH ( $n=4$ ). **(O)** Experimental timeline for treatment with Tilorone, an IFN agonist, in combination with NTG to assess its effects on pain sensitivity (red triangle) in WT mice injected with AAVs. **(P–Q)** Basal and acute mechanical paw withdrawal thresholds measured by von Frey filament in response to mechanical stimuli in mice treated with saline + mCherry, NTG + mCherry, NTG + shRNA, and NTG + shRNA + Tilorone ( $n=12–14$ ). The data are shown as mean  $\pm$  SEM, \* $p < 0.05$ , \*\* $p < 0.01$ , \*\*\*\* $p < 0.0001$ ; one-way ANOVA in **(I, N)**, two-way ANOVA in **(P, Q)**

behaviors, particularly in more stressful environments of the EPM. To investigate whether the IFN signaling pathway also influences chronic migraine-induced anxiety-like behaviors, we tested shRNA mice with NTG-treated along with either saline or tilorone injection. Unexpectedly, no significant differences were observed in either the OFT or the EPM test (Supplementary Fig. 8).

Overall, these data suggest that IDO1 in the ACC modulates anxiety-like behaviors related to chronic migraine. However, this modulation does not appear to be mediated through the IFN signaling pathway downstream of IDO1.

## Discussion

In this study, we utilized pharmacological inhibition, genetic knockout and AAV-mediated knockdown approaches to elucidate the pivotal role of IDO1 in pain sensitivity associated with chronic migraine and its underlying mechanism in the ACC. We evaluated neuronal activity in the ACC, a region linked to IDO1-mediated pain sensitivity, and found that ablation of IDO1 in the ACC effectively rescued electrophysiological E/I balance changes and mitigated migraine-related behaviors. Furthermore, we demonstrated that IDO1 in the ACC regulates microglial activation and synaptic pruning, influencing chronic migraine through the IFN signaling pathway. Thus, our study revealed that IDO1 regulates microglial pruning of neuronal synapses, thereby altering the E/I balance in the ACC, which affects pain sensitivity and anxiety-like behavior in chronic migraine model mice.

Emerging clinical imaging studies have demonstrated that ACC activity is involved in various types of pain-related information processing in the human brain and is also closely associated with the affective component of pain [44–47]. However, the relationship between ACC neuron activity and pain sensitization in chronic migraine remains poorly understood. In our study, immunofluorescence staining for c-Fos in whole-brain slices revealed robust expression of c-Fos<sup>+</sup> in the ACC of chronic migraine model mice. Notably, ACC neurons are known to respond to both noxious and nonnoxious

mechanical or thermal somatosensory stimuli, with pyramidal neurons being particularly responsive to noxious inputs [48]. Therefore, we monitored real-time sensory stimulus-induced compound Ca<sup>2+</sup> activity via the fiber photometry technique, and observed a significant increase in Ca<sup>2+</sup> signaling in the pyramidal neurons of the ACC in response to von Frey filament stimuli in NTG-treated mice, suggesting a correlation between these neurons and migraine hyperalgesia. Consistently, optogenetic studies have shown that specific activation of ACC pyramidal neurons reduces mechanical pain thresholds in mice with inflammatory pain [49], whereas inhibition of excitatory transmission produces analgesic effects in different chronic pain models [50, 51]. Similar results were obtained from complete Freund's adjuvant-treated mice under persistent pain [52]. Our electrophysiology results further revealed an increase in excitatory synaptic transmission in chronic migraine model mice, with no significant difference in inhibitory synaptic transmission or intrinsic membrane properties. Together, these results suggest that the enhancement of ACC neuronal activity following NTG-induced chronic migraine is due primarily to a shift in the E/I balance toward excitation.

Studies have indicated that metabolites produced in the serotonin and kynurenine pathways are associated with migraine [15, 16, 53]. IDO1 catalyzes the first and rate-limiting step in the tryptophan catabolism pathway, leading to the production of kynurenine and a consequent reduction in serotonin levels. While there is limited evidence suggesting a role for IDO1 in pain, its involvement in migraine remains unclear. In our study, we demonstrated that pharmacological inhibition, genetic knockout and AAV-mediated knockdown of IDO1 significantly alleviated pain hypersensitivity in a chronic migraine mouse model. 1-MT, IDO-specific competitive protein inhibitors, can effectively inhibit IDO1 activity. Treatment with 1-MT significantly attenuated nociceptive behaviors in neuropathic pain and chronic arthritis inflammatory pain [23, 25, 54], in accordance with our results. This finding aligns with a previous study showing that pharmacological inhibition of IDO1 attenuated pain hypersensitivity in neuropathic pain, likely through

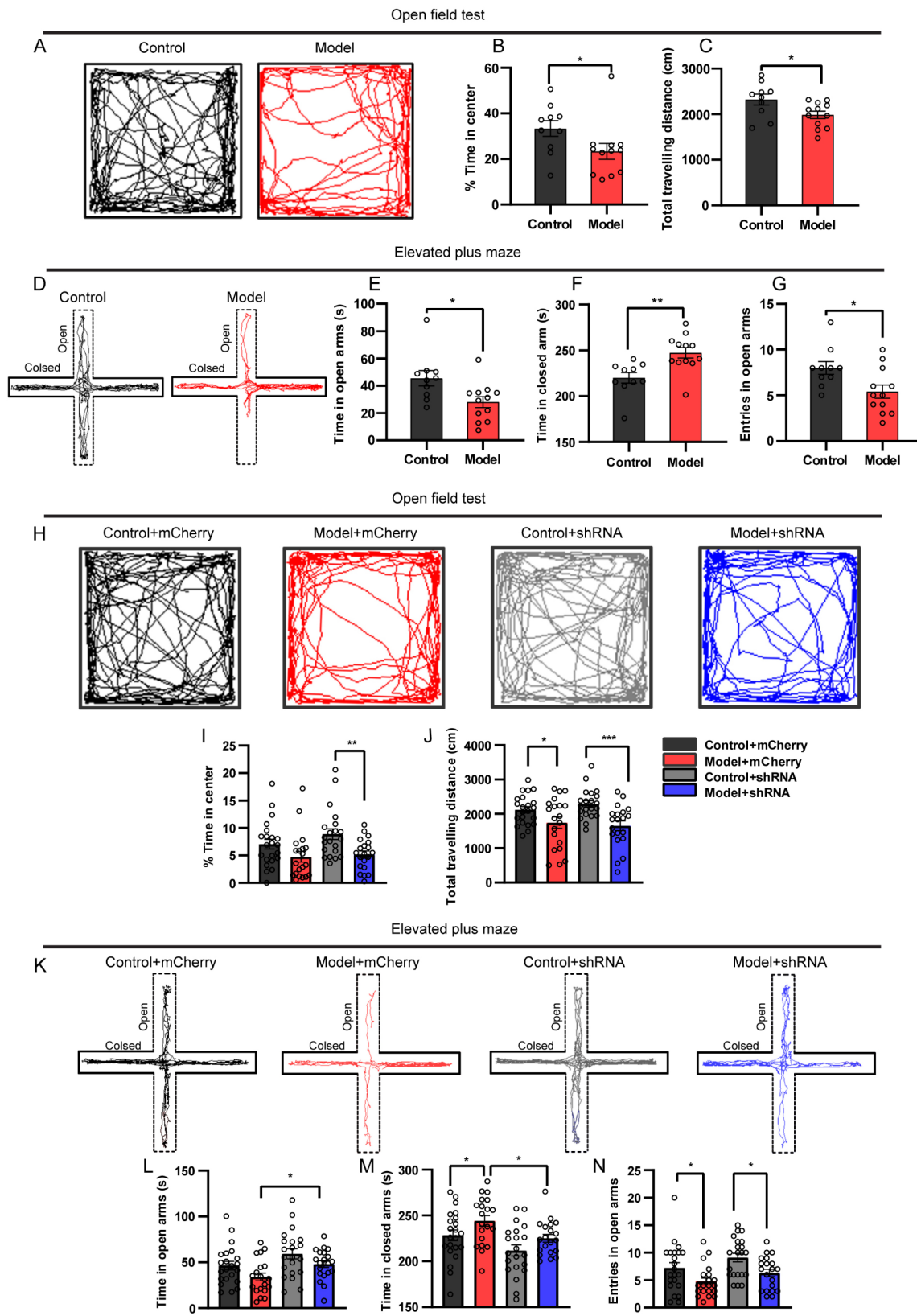


**Fig. 6** (See legend on next page.)

(See figure on previous page.)

**Fig. 6** IDO1 in the ACC modulates anxiety-like behaviors associated with chronic migraine. **(A–C)** Locomotor activity and time spent in the center in the OFT ( $n = 10–12$ ). **(D–G)** The time spent in open and closed arms, and the number of entries into open arms in the EPM ( $n = 10–12$ ). **(H–J)** Locomotor activity and time spent in the center in the OFT ( $n = 20–22$ ). **(K–N)** The time spent in open and closed arms, and the number of entries into open arms in the EPM ( $n = 20–22$ ). The data are shown as mean  $\pm$  SEM, \* $p < 0.05$ , \*\* $p < 0.01$ , \*\*\* $p < 0.001$ ; Student's *t* test in **(C, F)**, Mann-Whitney *U* test in **(B, E, G)**, one-way ANOVA in **(I, J, L–N)**

mechanisms involving synaptic plasticity and suppression of NMDA receptor activity [24]. To investigate whether changes in IDO1 levels alter synaptic function, we performed electrophysiological studies and found that the E/I imbalance observed in NTG-treated mice could be rescued by genetic knockout of IDO1. These results reveal the critical role of IDO1 in the ACC in regulating pain hypersensitivity in chronic migraine by modulating the E/I balance mechanism.

Several preclinical models of migraine have been extensively described. In this study, we selected four commonly used migraine models. NTG, a nitric oxide donor known to mediate migraine effects, is the most widely studied and considered one of the most reliable and reproducible models [55]. Studies in conscious mice reveal that systemic NTG induces migraine-related hyperalgesia [56] and similarly, our results also demonstrate that NTG significantly increases hind-paw mechanical and thermal hypersensitivity in mice. CSD, a slowly propagating wave of neuronal depolarization with glial and vascular activation, followed by neuronal suppression, mimics phenomena associated with migraine aura [57]. The CSD-induced murine migraine models presented facial hyperalgesia, photophobia and hypomotility, which could be reversed by acute anti-migraine drugs [58]. ES of meningeal nerve terminals innervating the superior sagittal sinus to elicit trigeminal afferent activation has also been used to model migraine preclinically [59]. ES-treated mice exhibited significant mechanical allodynia, which is the most common pain-like behavior in migraine models [60]. Serotonin plays a key role in migraine pathophysiology, and reserpine, a monoamine depletor, increases sensitivity to nitric oxide-induced cerebral microvessel dilation and leads to a migraine-like phenotype. In our study, we found a significant elevated levels of IDO1 in all four models of chronic migraine, highlighting the important role of IDO1 in chronic migraine, rather than in NTG-induced chronic migraine.

Microglial activation has been implicated in animal models of pain sensitization, such as inflammatory pain, neuropathic pain and chronic pain [61–63]. IDO1 is also known to participate in immunometabolism and inflammatory programming via its role in tryptophan catabolism, suggesting a potential regulatory role of IDO1 in chronic migraine through microglial activation. Our results showed coexpression of IDO1 and IBA1 in microglia, with significantly increased numbers of coexpressing cells in chronic migraine mice. Genetic knockout

of IDO1 reversed the microglial activation and associated changes in cell number and morphology in the ACC. A recent study demonstrated that the activation of microglia in the ACC is involved in mechanical allodynia in mice with neuropathic pain [64], a mechanism that may be relevant to our findings. In addition, microglia play a crucial role in synapse pruning. A previous study reported that chronic psychological stress induces microglial activation in the amygdala, contributing to visceral hypersensitivity via synaptic engulfment, and that blocking C1q/C3-CR3 signaling can attenuate this hypersensitivity [65]. Early-life inflammation has also been shown to contribute to depressive-like behaviors via Cx3Cr1-mediated microglial phagocytosis of synapses around the ACC in adolescence [66]. Similarly, we observed that NTG treatment induced excessive microglial phagocytosis in the ACC, while IDO1 knockout mice displayed a significant reduction in synaptic pruning, resulting in greater resilience to chronic migraine. Surprisingly, our immunofluorescence staining, combined with the electrophysiology results, revealed increased excitatory synaptic transmission and microglia-mediated synaptic pruning (based on Syn1 and IBA1 immunostaining) in NTG-treated mice, both of which were reversed by IDO1 knockout. These findings suggest that synaptic pruning may be a concomitant phenomenon under inflammatory conditions in chronic migraine. Collectively, our results highlight the important role of IDO1 in regulating microglial activation in chronic migraine, and manipulation of IDO1 can reduce microglia-mediated synaptic pruning, and alleviate pain hypersensitivity.

To further elucidate the mechanisms by which IDO1 regulates chronic migraine, we investigated the signaling pathways involved in IDO1-mediated microglial activation and alterations in the E/I balance. Despite ongoing research, the specific pathways involved remain incompletely understood. Our RNA sequencing analysis revealed that the IFN signaling pathway is responsive in chronic migraine models. Previous studies have indicated that IFN acts upstream of IDO1, promoting its expression [67, 68]. However, our findings suggest that IFN may also function downstream of IDO1. Specifically, the administration of an IFN agonist reversed the alleviation of pain hypersensitivity observed in chronic migraine model mice with AAV-mediated IDO1 knockdown. These findings suggest a potential synergistic relationship between IDO1 and IFN. In addition, IFN, especially IFN- $\gamma$ , has been shown to induce sustained microglial activation,

including microglial proliferation and enhanced synapse elimination [69], resulting in detrimental neuroinflammation and abnormal synaptic transmission [70]. Our study provides evidence that IDO1 regulates microglial activation via the IFN signaling pathway, contributing to the pain hypersensitivity associated with chronic migraine.

Prolonged migraine attacks are associated with a range of psychiatric comorbidities, with anxiety and depression being the most prevalent in chronic migraine patients [71]. Approximately half of migraine sufferers experience anxiety, while 20% experience depression [72]. Consistent with these findings, we observed reduced locomotor activity and anxiety-like behaviors in chronic migraine model mice. However, no significant difference was found in the SPT or FST, suggesting that anxiety, rather than depression, is more commonly associated with chronic migraine in the NTG mouse model, which aligns with clinical evidence. Previous studies have reported that the ACC mediates comorbid emotional disorders in chronic pain [43, 73]. Additionally, increased IDO1 activity in neuroinflammation leads to a deficiency in serotonin synthesis, potentially triggering psychiatric disorders [74, 75]. However, the role of ACC IDO1 in anxiety-like behaviors associated with chronic migraine remains unclear. In our study, knockdown of IDO1 in the ACC partially rescued anxiety-like behavior, as evidenced by changes in time spent in the open arms and closed arms of the EPM test but not in the time spent in the center zone of the OFT. This contradictory result may be due to the open, elevated apparatus of the EPM, which induces higher levels of fear and risk assessment compared to the OFT [76]. Since our results revealed that IDO1 modulates pain sensitization through the IFN signaling pathway in chronic migraine, we hypothesized that interfering with IFN signaling might affect anxiety-like behavior. Unexpectedly, IDO1 knockdown in chronic migraine model mice did not affect anxiety-like behavior, regardless of treatment with an IFN agonist or saline, suggesting that IDO1 influences pain sensitization, but not anxiety-like behavior, through IFN signaling.

The present study has a certain limitation. Gender differences exist in chronic migraine and to avoid the effects of estrogen on pain mediator transmission [77], male mice were employed to establish the chronic migraine model. Therefore, future studies in female mice will be required to investigate sex differences in migraine pathogenesis.

## Conclusion

In summary, our study revealed the pivotal role of IDO1 in the pathophysiology of chronic migraine and its associated psychiatric comorbidities, particularly in relation to microglial function and synaptic integrity. These

findings suggest that targeting IDO1 and its related pathways, such as IFN signaling, may offer novel therapeutic strategies for chronic migraine.

## Abbreviations

IDO1	Indoleamine 2,3-dioxygenase 1
NTG	Nitroglycerin
ACC	Anterior cingulate cortex
E/I	Excitation/inhibition
IFN	Interferon
Syn1	Synapsin1
PSD95	Postsynaptic density protein 95
KO	Knockout
WT	Wild-type
CSD	Cortical spreading depression
ES	Electrical stimulation
1-MT	1-methyltryptophan
PBS	Phosphate-buffered saline
OFT	Open field test
EPM	Elevated plus maze test
SPT	Sucrose preference test
FST	Forced swimming test
cDNA	Complementary deoxyribonucleic acid
ANOVA	Analysis of variance
AAV	Adeno-associated virus
shRNA	Short hairpin RNA
mCherry	mCherry fluorescent protein
CaMKII	Ca <sup>2+</sup> -dependent protein kinases II
GCaMP	GFP-calmodulin-M13 peptide
sEPSCs	Spontaneous excitatory postsynaptic currents
sIPSCs	Spontaneous inhibitory postsynaptic currents
RMP	Resting membrane potential
R <sub>in</sub>	input resistance
AP	Action potential
PCA	Principal component analysis
DEGs	Differentially expressed genes
GO	Gene Ontology
KEGG	The Kyoto Encyclopedia of Genes and Genomes
GSEA	Gene Set Enrichment Analysis
OFC	Orbitofrontal cortex
mPFC	Medial prefrontal cortex
M1	Primary motor cortex
M2	Secondary motor cortex
S1	Primary somatosensory cortex
BLA	Basolateral amygdala
PH	Posterior hypothalamic area
PV	Paraventricular thalamic nucleus
PAG	Periaqueductal gray

## Supplementary Information

The online version contains supplementary material available at <https://doi.org/10.1186/s12974-025-03367-w>.

Supplementary Material 1

Supplementary Material 2

## Acknowledgements

Not applicable.

## Author contributions

W.-P. L. and J. H. performed electrophysiological recordings, fiber photometry behavioral experiments and analysis. J. H. performed the behavioral experiments, virus injections, immunofluorescence staining and western blotting with the help of W.-J. J., G.-Y. L., X.-H. S., J.-M. Z., Y. H. and Y.-F. X. Y.-Y. Z. and W. X. supervised all phases of the project. All authors contributed to interpretation of the results, and W. X., W.-P. L. and J. H. assembled the figures and wrote the paper. All authors read and approved the final manuscript.

## Funding

This study was supported by the National Natural Science Foundation of China (Grant No. 82374193, 81873158), the China Postdoctoral Science Foundation (Grant No. 2022M720061), Guangdong Basic and Applied Basic Research Foundation (Grant No. 2023A1515220030, 2023A1515110505, 2021A1515110231), The second national famous Traditional Chinese Medicine Inheritance Studio (Grant No. G724290126) and the Key Discipline Construction Project of Traditional Chinese Medicine of Guangdong Province (Grant No. 20220105).

## Data availability

The data that support the findings of this study are available from the corresponding author upon reasonable request.

## Declarations

### Ethical approval

All animal experimental procedures were approved by the Institutional Animal Care and Use Committee of Southern Medical University (L-2019-071, Guangdong, China).

### Consent for publication

Not applicable.

### Competing interests

The authors declare no competing interests.

### Author details

<sup>1</sup>School of Traditional Chinese Medicine, Southern Medical University, Guangzhou 510515, China

<sup>2</sup>Guangdong Basic Research Center of Excellence for Integrated Traditional and Western Medicine for Qingzhi Diseases, Guangzhou 510515, China

<sup>3</sup>Department of Neurology, The Third Affiliated Hospital of Sun Yat-Sen University, Guangzhou 510630, China

<sup>4</sup>Department of Critical Care Medicine, The Affiliated Traditional Chinese Medicine Hospital of Guangzhou Medical University, Guangzhou 510130, China

<sup>5</sup>Department of Neurology, Southern Medical University Hospital of Integrated Traditional Chinese and Western Medicine, Southern Medical University, Guangzhou 510317, China

Received: 4 November 2024 / Accepted: 3 February 2025

Published online: 18 February 2025

## References

- Headache Classification Committee of the International Headache Society (IHS) The International Classification of Headache Disorders, 3rd edition. Cephalalgia. 2018; 38.
- Ferrari MD, Goadsby PJ, Burstein R, Kurth T, Ayata C, Charles A, Ashina M, van den Maagdenberg AMJM, Dodick DW. Migraine. Nat Rev Dis Primers. 2022;8:2.
- Global regional. National burden of disorders affecting the nervous system, 1990–2021: a systematic analysis for the global burden of Disease Study 2021. Lancet Neurol. 2024;23:344–81.
- Burch RC, Buse DC, Lipton RB. Migraine: Epidemiology, Burden, and Comorbidity. Neurol Clin. 2019;37:631–49.
- Peres MFP, Mercante JPP, Toba PR, Kamei H, Bigal ME. Anxiety and depression symptoms and migraine: a symptom-based approach research. J Headache Pain. 2017;18:37.
- Buse DC, Silberstein SD, Manack AN, Papapetropoulos S, Lipton RB. Psychiatric comorbidities of episodic and chronic migraine. J Neurol. 2013;260:1960–9.
- Della Pietra A, Mikhailov N, Giniatullin R. FM1-43 dye memorizes Piezo1 activation in the trigeminal nociceptive system implicated in Migraine Pain. Int J Mol Sci. 2023; 24.
- Tzeng H, Lee MT, Fan P, Knutson DE, Lai T, Sieghart W, Cook J, Chiou L.  $\alpha$ 6GABA receptor positive modulators alleviate migraine-like grimaces in mice via compensating GABAergic deficits in trigeminal ganglia. Neurotherapeutics. 2021;18:569–85.
- Yang DG, Gao YY, Yin ZQ, Wang XR, Meng XS, Zou TF, Duan YJ, Chen YL, Liao CZ, Xie ZL, et al. Roxadustat alleviates nitroglycerin-induced migraine in mice by regulating HIF-1 $\alpha$ /NF- $\kappa$ B/inflammation pathway. Acta Pharmacol Sin. 2023;44:308–20.
- Jing F, Zhang YX, Long T, He W, Qin GC, Zhang DK, Chen LX, Zhou JY. P2Y12 receptor mediates microglial activation via RhoA/ROCK pathway in the trigeminal nucleus caudalis in a mouse model of chronic migraine. J Neuroinflamm. 2019;16:217.
- Bushnell MC, Ceko M, Low LA. Cognitive and emotional control of pain and its disruption in chronic pain. Nat Rev Neurosci. 2013;14:502–11.
- Christensen RH, Ashina H, Al-Khazali HM, Zhang Y, Tolnai D, Poulsen AH, Cagol A, Hadjikhani N, Granziera C, Amin FM, et al. Differences in cortical morphology in people with and without migraine: a Registry for Migraine (REFORM) MRI study. Neurology. 2024;102:e209305.
- Hougaard A, Amin FM, Arrngrim N, Vlachou M, Larsen VA, Larsson HBW, Ashina M. Sensory migraine aura is not associated with structural grey matter abnormalities. Neurolmage Clin. 2016;11:322–7.
- Hubbard CS, Khan SA, Keaser ML, Mathur VA, Goyal M, Seminowicz DA. Altered brain structure and function correlate with Disease Severity and Pain Catastrophizing in Migraine patients. eNeuro. 2014;1:e14–20.
- Curto M, Lionetto L, Negro A, Capi M, Fazio F, Giamberardino MA, Simmaco M, Nicoletti F, Martelletti P. Altered kynurenine pathway metabolites in serum of chronic migraine patients. J Headache Pain. 2015;17:47.
- Tuka B, Nyári A, Cseh EK, Körtési T, Veréb D, Tömösi F, Kecskeméti G, Janáky T, Tajti J, Vécsei L. Clinical relevance of depressed kynurenine pathway in episodic migraine patients: potential prognostic markers in the peripheral plasma during the interictal period. J Headache Pain. 2021;22:60.
- Pallotta MT, Rossini S, Suvieri C, Coletti A, Orabona C, Macchiarulo A, Volpi C, Grohmann U. Indoleamine 2,3-dioxygenase 1 (IDO1): an up-to-date overview of an eclectic immunoregulatory enzyme. FEBS J. 2022;289:6099–118.
- Jovanovic F, Candido KD, Knezevic NN. The role of the Kynurenine Signaling Pathway in different Chronic Pain conditions and potential use of Therapeutic agents. Int J Mol Sci. 2020; 21.
- Palego L, Betti L, Rossi A, Giannaccini G. Tryptophan Biochemistry: Structural, Nutritional, Metabolic, and Medical Aspects in Humans. J Amino Acids. 2016; 2016: 8952520.
- Sodhi RK, Bansal Y, Singh R, Saroj P, Bhandari R, Kumar B, Kuhad A. IDO-1 inhibition protects against neuroinflammation, oxidative stress and mitochondrial dysfunction in 6-OHDA induced murine model of Parkinson's disease. Neurotoxicology. 2021;84:184–97.
- Duan ZZ, Shi L, He ZNT, Kuang CX, Han TX, Yang Q. The protective effect of IDO1 inhibition in A $\beta$ -Treated neurons and APP/PS1 mice. Am J Alzheimers Dis Other Dement. 2023;38:250574093.
- Deng N, Hu J, Hong Y, Ding YW, Xiong YF, Wu ZY, Xie W. Indoleamine-2,3-Dioxygenase 1 Deficiency suppresses seizures in Epilepsy. Front Cell Neurosci. 2021;15:638854.
- Maganin AG, Souza GR, Fonseca MD, Lopes AH, Guimarães RM, Dagostin A, Cecilio NT, Mendes AS, Gonçalves WA, Silva CE et al. Meningeal dendritic cells drive neuropathic pain through elevation of the kynurenine metabolic pathway in mice. J Clin Invest. 2022; 132.
- Wang Y, Li CM, Han R, Wang ZZ, Gao YL, Zhu XY, Yu X, Du GY, Wang HB, Tian JW, et al. PCCO208009, an indirect IDO1 inhibitor, alleviates neuropathic pain and co-morbidities by regulating synaptic plasticity of ACC and amygdala. Biochem Pharmacol. 2020;177:113926.
- Rojewska E, Ciapala K, Piotrowska A, Makuch W, Mika J. Pharmacological inhibition of indoleamine 2,3-Dioxygenase-2 and kynurenine 3-Monooxygenase, enzymes of the Kynurenine Pathway, significantly diminishes Neuropathic Pain in a rat model. Front Pharmacol. 2018;9:724.
- Xie W, Cai L, Yu YH, Gao L, Xiao LM, He QC, Ren ZJ, Liu YZ. Activation of brain indoleamine 2,3-dioxygenase contributes to epilepsy-associated depressive-like behavior in rats with chronic temporal lobe epilepsy. J Neuroinflamm. 2014;11:41.
- Ekins S, Lingerfelt MA, Comer JE, Freiberg AN, Mirsalis JC, O'Loughlin K, Harutyunyan A, McFarlane C, Green CE, Madrid PB. Efficacy of Tilorone Dihydrochloride against Ebola Virus infection. Antimicrob Agents Chemother. 2018; 62.
- Pradhan AA, Smith ML, Mcguire B, Tarash I, Evans CJ, Charles A. Characterization of a novel model of chronic migraine. Pain. 2014;155:269–74.
- Donmez-Demir B, Erdener SE, Karatas H, Kaya Z, Ulusoy I, Dalkara T. KCl-induced cortical spreading depression waves more heterogeneously propagate than optogenetically-induced waves in lissencephalic brain: an analysis with optical flow tools. Sci Rep. 2020;10:12793.

30. Dong Z, Jiang L, Wang XH, Wang XL, Yu SY. Nociceptive behaviors were induced by electrical stimulation of the dura mater surrounding the superior sagittal sinus in conscious adult rats and reduced by morphine and rizatriptan benzoate. *Brain Res.* 2011;1368:151–8.
31. Pu ZH, Peng C, Xie XF, Luo M, Zhu H, Feng R, Xiong L. Alkaloids from the rhizomes of *Ligusticum striatum* exert antimigraine effects through regulating 5-HT<sub>1B</sub> receptor and c-Jun. *J Ethnopharmacol.* 2019;237:39–46.
32. Chaplan SR, Bach FW, Pogrel JW, Chung JM, Yaksh TL. Quantitative assessment of tactile allodynia in the rat paw. *J Neurosci Methods.* 1994;53:55–63.
33. Vong CT, Chen YL, Chen ZJ, Gao CF, Yang FQ, Wang SP, Wang YT. Classical prescription Dachuanxiong Formula delays nitroglycerin-induced pain response in migraine mice through reducing endothelin-1 level and regulating fatty acid biosynthesis. *J Ethnopharmacol.* 2022;288:114992.
34. Su XH, Li WP, Wang YJ, Liu J, Liu JY, Jiang Y, Peng FH. Chronic administration of 13-cis-retinoic acid induces Depression-Like Behavior by altering the activity of Dentate Granule cells. *Neurotherapeutics.* 2022;19:421–33.
35. Li WP, Su XH, Hu NY, Hu J, Li XW, Yang JM, Gao TM. Astrocytes mediate cholinergic regulation of adult hippocampal neurogenesis and memory through M1 muscarinic receptor. *Biol Psychiatry.* 2022;92:984–98.
36. Schafer DP, Lehrman EK, Heller CT, Stevens B. An engulfment assay: a protocol to assess interactions between CNS phagocytes and neurons. *J Vis Exp.* 2014.
37. Yao DD, Chen YR, Chen G. The role of pain modulation pathway and related brain regions in pain. *Rev Neurosci.* 2023;34:899–914.
38. Biswas K. Microglia mediated neuroinflammation in neurodegenerative diseases: a review on the cell signaling pathways involved in microglial activation. *J Neuroimmunol.* 2023;383:578180.
39. Wu YW, Dissing-Olesen L, Macvicar BA, Stevens B, Microglia. Dynamic mediators of Synapse Development and Plasticity. *Trends Immunol.* 2015;36:605–13.
40. Hong S, Beja-Glasser VF, Nfonoyim BM, Frouin A, Li S, Ramakrishnan S, Merry KM, Shi Q, Rosenthal A, Barres BA, et al. Complement and microglia mediate early synapse loss in Alzheimer mouse models. *Science.* 2016;352:712–6.
41. Kopitar-Jerala N. The role of interferons in inflammation and inflammasome activation. *Front Immunol.* 2017;8:873.
42. Barthas F, Sellmeijer J, Hugel S, Waltsperger E, Barrot M, Yalcin I. The anterior cingulate cortex is a critical hub for pain-induced depression. *Biol Psychiatry.* 2015;77:236–45.
43. Koga K, Descalzi G, Chen T, Ko HG, Lu JS, Li S, Son JH, Kim T, Kwak C, Haganir RL, et al. Coexistence of two forms of LTP in ACC provides a synaptic mechanism for the interactions between anxiety and chronic pain. *Neuron.* 2015;85:377–89.
44. Caston RM, Smith EH, Davis TS, Singh R, Rahimpour S, Rolston JD. Psychophysical pain encoding in the cingulate cortex predicts responsiveness of electrical stimulation. *medRxiv [Preprint];* 2023.
45. Xiong HY, Cao YQ, Du SH, Yang QH, He SY, Wang XQ. Effects of High-Definition Transcranial Direct Current Stimulation Targeting the Anterior Cingulate Cortex on the Pain thresholds: a Randomized Controlled Trial. *Pain Med.* 2023;24:89–98.
46. Wang Y, Cao DY, Remeniuk B, Krimmel S, Seminowicz DA, Zhang M. Altered brain structure and function associated with sensory and affective components of classic trigeminal neuralgia. *Pain.* 2017;158:1561–70.
47. Chen B, He Y, Xia L, Guo LL, Zheng JL. Cortical plasticity between the pain and pain-free phases in patients with episodic tension-type headache. *J Headache Pain.* 2016;17:105.
48. Koga K, Li XY, Chen T, Steenland HW, Descalzi G, Zhuo M. In vivo whole-cell patch-clamp recording of sensory synaptic responses of cingulate pyramidal neurons to noxious mechanical stimuli in adult mice. *Mol Pain.* 2010;6:62.
49. Kang SJ, Kwak C, Lee J, Sim S, Shim J, Choi T, Collingridge GL, Zhuo M, Kaang B. Bidirectional modulation of hyperalgesia via the specific control of excitatory and inhibitory neuronal activity in the ACC. *Mol Brain.* 2015;8:81.
50. Li XY, Ko HG, Chen T, Descalzi G, Koga K, Wang HS, Kim SS, Shang YZ, Kwak C, Park SW, et al. Alleviating neuropathic pain hypersensitivity by inhibiting PKMzeta in the anterior cingulate cortex. *Science.* 2010;330:1400–4.
51. Zhuo M. Long-term potentiation in the anterior cingulate cortex and chronic pain. *Philos Trans R Soc B Biol Sci.* 2014;369:20130146.
52. Tang HD, Dong WY, Hu R, Huang JY, Huang ZH, Xiong W, Xue T, Liu J, Yu JM, Zhu X, et al. A neural circuit for the suppression of feeding under persistent pain. *Nat Metab.* 2022;4:1746–55.
53. Vécsei L, Szalárdy L, Fülöp F, Toldi J. Kynurenines in the CNS: recent advances and new questions. *Nat Rev Drug Discov.* 2013;12:64–82.
54. Kim H, Chen L, Lim G, Sung B, Wang SX, McCabe MF, Rusanescu G, Yang LL, Tian YH, Mao JR. Brain indoleamine 2,3-dioxygenase contributes to the comorbidity of pain and depression. *J Clin Invest.* 2012;122:2940–54.
55. Sureda-Gibert P, Romero-Reyes M, Akerman S. Nitroglycerin as a model of migraine: clinical and preclinical review. *Neurobiol Pain.* 2022;12:100105.
56. Pradhan AA, Smith ML, Zyuzin J, Charles A.  $\delta$ -Opioid receptor agonists inhibit migraine-related hyperalgesia, aversive state and cortical spreading depression in mice. *Br J Pharmacol.* 2014;171:2375–84.
57. Kitamura E, Imai N. Molecular and Cellular Neurobiology of spreading Depolarization/Depression and migraine: a narrative review. *Int J Mol Sci.* 2024;25.
58. Tang C, Unekawa M, Kitagawa S, Takizawa T, Kayama Y, Nakahara J, Shibata M. Cortical spreading depolarisation-induced facial hyperalgesia, photophobia and hypomotility are ameliorated by sumatriptan and olcegepant. *Sci Rep.* 2020;10:11408.
59. Zagami AS, Goadsby PJ, Edvinsson L. Stimulation of the superior sagittal sinus in the cat causes release of vasoactive peptides. *Neuropeptides.* 1990;16:69–75.
60. Zhang Y, Wang H, Sun YF, Huang ZT, Tao Y, Wang YR, Jiang XH, Tao J. Trace amine-associated receptor 1 regulation of Kv1.4 channels in trigeminal ganglion neurons contributes to nociceptive behaviors. *J Headache Pain.* 2023;24:49.
61. Chen G, Zhang YQ, Qadri YJ, Serhan CN, Ji RR. Microglia in Pain: detrimental and protective roles in Pathogenesis and Resolution of Pain. *Neuron.* 2018;100:1292–311.
62. Zhao H, Alam A, Chen Q, A Eusman M, Pal A, Eguchi S, Wu L, Ma D. The role of microglia in the pathobiology of neuropathic pain development: what do we know? *Br J Anaesth.* 2017;118:504–16.
63. He W, Wang YY, Zhang YX, Zhang YN, Zhou JY. The status of knowledge on migraines: the role of microglia. *J Neuroimmunol.* 2023;381:578118.
64. Miyamoto K, Kume K, Ohsawa M. Role of microglia in mechanical allodynia in the anterior cingulate cortex. *J Pharmacol Sci.* 2017;134:158–65.
65. Wang J, Chen HS, Li HH, Wang HJ, Zou RS, Lu XJ, Wang J, Nie BB, Wu JF, Li S, et al. Microglia-dependent excessive synaptic pruning leads to cortical underconnectivity and behavioral abnormality following chronic social defeat stress in mice. *Brain Behav Immun.* 2023;109:23–36.
66. Cao P, Chen CM, Liu A, Shan QH, Zhu X, Jia CH, Peng XQ, Zhang M, Farzinpour Z, Zhou WJ et al. Early-life inflammation promotes depressive symptoms in adolescence via microglial engulfment of dendritic spines. *Neuron.* 2021; 109.
67. Sundaram K, Mu JY, Kumar A, Behera J, Lei C, Sriwastva MK, Xu FY, Fryden GW, Zhang LF, Chen SY, et al. Garlic exosome-like nanoparticles reverse high-fat diet induced obesity via the gut/brain axis. *Theranostics.* 2022;12:1220–46.
68. Yang SL, Tan HX, Niu TT, Liu YK, Gu CJ, Li DJ, Li MQ, Wang HY. The IFN- $\gamma$ -IDO1-kynurenic pathway-induced autophagy in cervical cancer cell promotes phagocytosis of macrophage. *Int J Biol Sci.* 2021;17:339–52.
69. Kann O, Almouhanna F, Chausse B. Interferon  $\gamma$ : a master cytokine in microglia-mediated neural network dysfunction and neurodegeneration. *Trends Neurosci.* 2022;45:913–27.
70. Wangler LM, Godbout JP. Microglia moonlighting after traumatic brain injury: aging and interferons influence chronic microglia reactivity. *Trends Neurosci.* 2023;46:926–40.
71. Minen MT, De Begasse O, Van Kroon A, Powers S, Schwedt TJ, Lipton R, Silbersweig D. Migraine and its psychiatric comorbidities. *J Neurol Neurosurg Psychiatry.* 2016;87:741–9.
72. Devlen J. Anxiety and depression in migraine. *J R Soc Med.* 1994;87:338–41.
73. Ren D, Li JN, Qiu XT, Wan FP, Wu ZY, Fan BY, Zhang MM, Chen T, Li H, Bai Y, et al. Anterior cingulate cortex mediates hyperalgesia and anxiety Induced by Chronic Pancreatitis in rats. *Neurosci Bull.* 2022;38:342–58.
74. Jeon SW, Kim Y. Inflammation-induced depression: its pathophysiology and therapeutic implications. *J Neuroimmunol.* 2017;313:92–8.
75. Catena-Dell'Osso M, Rotella F, Dell'Osso A, Fagioli A, Marazziti D. Inflammation, serotonin and major depression. *Curr Drug Targets.* 2013;14:571–7.
76. Carola V, D'Olimpio F, Brunamonti E, Mangia F, Renzi P. Evaluation of the elevated plus-maze and open-field tests for the assessment of anxiety-related behaviour in inbred mice. *Behav Brain Res.* 2002;134:49–57.
77. Marcus R. Study provides New Insight into Female Sex hormones and migraines. *JAMA.* 2023;329:1439–40.

## Publisher's note

Springer Nature remains neutral with regard to jurisdictional claims in published maps and institutional affiliations.